Zoosyst. Evol. 96 (1) 2020, 217–236 | DOI 10.3897/zse.96.50821

PENSOFT

MUSEUM FÜR NATURKUNDE BERLIN

Small is beautiful: the first phylogenetic analysis of *Bryodelphax* Thulin, 1928 (Heterotardigrada, Echiniscidae)

Piotr Gąsiorek[1], Katarzyna Vončina[1], Peter Degma[2], Łukasz Michalczyk[1]

1 *Institute of Zoology and Biomedical Research, Jagiellonian University, Gronostajowa 9, 30-387, Kraków, Poland*

2 *Department of Zoology, Faculty of Natural Sciences, Comenius University in Bratislava, Mlynská dolina, Ilkovičova 6/B1, 84215, Bratislava, Slovakia*

http://zoobank.org/0B80FF1B-5ED7-430B-A471-A5DE02E8E6D3

Corresponding author: Piotr Gąsiorek (piotr.lukas.gasiorek@gmail.com)

Academic editor: Martin Husemann ♦ **Received** 10 February 2020 ♦ **Accepted** 17 April 2020 ♦ **Published** 27 May 2020

Abstract

The phyletic relationships both between and within many of tardigrade genera have been barely studied and they remain obscure. Amongst them is the cosmopolitan *Bryodelphax*, one of the smallest in terms of body size echiniscid genera. The analysis of newly-found populations and species from the Mediterranean region and from South-East Asia gave us an opportunity to present the first phylogeny of this genus, which showed that phenotypic traits used in classical *Bryodelphax* taxonomy do not correlate with their phyletic relationships. In contrast, geographic distribution of the analysed species suggests their limited dispersal abilities and seems to be a reliable predictor of phylogenetic affinities within the genus. Moreover, we describe three new species of the genus. *Bryodelphax australasiaticus* **sp. nov.**, by having the ventral plate configuration VII:4-4-2-4-2-2-1, is a new member of the *weglarskae* group with a wide geographic range extending from the Malay Peninsula through the Malay Archipelago to Australia. *Bryodelphax decoratus* **sp. nov.** from Central Sulawesi (Celebes) also belongs to the *weglarskae* group (poorly visible ventral plates VII:4-2-2-4-2-2-1) and is closely related to the recently described *Bryodelphax arenosus* Gąsiorek, 2018, but is differentiated from the latter by well-developed epicuticular granules on the dorsum. Finally, a new dioecious species, *Bryodelphax nigripunctatus* **sp. nov.**, is described from Mallorca and, by the reduced ventral armature (II/III:2-2-(1)), it resembles *Bryodelphax maculatus* Gąsiorek et al., 2017. The latter species, known so far only from northern Africa, is recorded from Europe for the first time. A taxonomic key to the genus members is also presented.

Key Words

cradle hypothesis, Everything is Everywhere hypothesis, geographic distribution, miniaturisation, phylogeny, ventral plates

Introduction

Tardigrades are regarded as miniaturised panarthropods (Gross et al. 2019). The average body size of a limno-terrestrial tardigrade varies between 200 and 500 µm, with some notable exceptions, such as milnesiids (Morek et al. 2016) or richtersiids (Guidetti et al. 2016), reaching body lengths up to 1200 µm (Nelson et al. 2015). Marine heterotardigrades are the smallest representatives of the phylum, being usually below 200 µm in body length (Jørgensen et al. 2014; Fontoura et al. 2017), but speciose heterotardigrade echiniscids fit to the aforementioned range for limno-terrestrial water bears (200–500 µm), with single exceptions, such as *Acanthechiniscus islandicus* (Richters, 1904) (Maucci 1996) and some members of the genus *Cornechiniscus* (Maucci 1979; Kristensen 1987), which can grow up to 800 µm. The opposite trend, i.e. a potential reduction of the already small body size in the course of evolution, can be seen in five indirectly related genera: *Antechiniscus*, *Bryodelphax*, *Parechiniscus*, *Pseudechiniscus* and *Stellariscus* (Kristensen 1987; Claxton 2001; Gąsiorek 2018; Gąsiorek et al. 2018a). Of these genera exhibiting small body size, all but *Bryodelphax* and *Parechiniscus* share black crystalline eyes and sexual reproduction (Kristensen 1987). Furthermore, *Bryodelphax* is unique amongst Echiniscidae as it exhibits some peculiar apomorphies (e.g. ten peribuccal papulae) and plesiomorphies (e.g. ancestral type of the buccal

apparatus). These characteristics make *Bryodelphax* a good example of mosaic evolution in tardigrades (Kristensen et al. 2010; Gąsiorek 2018).

The aim of this study was to elucidate the phylogeny of *Bryodelphax* in relation to morphological traits used in its taxonomy, with application of the integrative approach, i.e. DNA barcoding and both qualitative and quantitative morphology, based on three new species that are described and illustrated herein. Our analyses reveal no congruence between the topology of the phylogenetic tree and the traditional taxonomic divisions of the genus (based on the presence of ventral armature), the reproductive mode or the development of dark, contrasting epicuticular granules on the dorsal plates. On the other hand, we show that phylogeny is tightly correlated with geography. In addition, an amended and updated key to the genus *Bryodelphax* is provided.

Materials and methods

Sample collection and processing, comparative material

Specimens of the genus *Bryodelphax* were extracted from various moss and lichen samples collected in numerous European and Asian locales (details in Table 1). The animals were divided into three groups used in different analyses: (I) qualitative and quantitative morphology investigated in phase contrast microscopy (PCM) and Nomarski differential interference contrast microscopy (NCM), collectively termed as light contrast microscopy (LCM); (II) qualitative morphology in scanning electron microscopy (SEM); and (III) DNA sequencing (details in Table 2). For morphological comparisons, the type series of *B. aaseae* Kristensen et al., 2010, *B. amphoterus* (Durante Pasa & Maucci, 1975), *B. asiaticus* Kaczmarek & Michalczyk, 2004, *B. brevidentatus* Kaczmarek et al., 2005, *B. iohannis* Bertolani et al., 1996, *B. meronensis* Pilato et al., 2010, *B. parvuspolaris* Kaczmarek et al., 2012, *B. sinensis* (Pilato, 1974) and *B. weglarskae* (Pilato, 1972) deposited in the Natural History of Denmark, University of Modena and Reggio Emilia, Museum of Natural History of Verona, Jagiellonian University and University of Catania, were studied.

Microscopy, imaging and morphometrics

Permanent microscope slides were made using Hoyer's medium and examined under a Nikon Eclipse 50i PCM associated with a Nikon Digital Sight DS-L2 digital camera and Olympus BX51 PCM and DIC associated with a digital camera CCD ColorView III FW. Specimens for imaging in the SEM were prepared according to Stec et al. (2015) and examined in Versa 3D Dual-Beam SEM at the ATOMIN facility of the Jagiellonian University. All figures were assembled in Corel Photo-Paint X6, ver. 16.4.1.1281 or in Adobe Photoshop CS3 Extended, ver. 10.0. All measurements are given in micrometres (µm) and were performed under PCM. Structures were measured only when not broken, de-

Table 1. Collection data for the newly-sequenced species used in morphological and phylogenetic analyses.

Species	Sample code	Coordinates, altitude	Locality	Environment	Sample type, substrate	Collector
Bryodelphax australasiaticus sp. nov.	MY.240	5°27'05"N, 100°11'00"E, 4 m asl	Malaysia, Pulau Pinang, Pantai Keracut	beach dominated by *Casuarina equisetifolia*	moss, tree branch	Piotr Gąsiorek & Artur Oczkowski
	MY.241	5°27'05"N, 100°11'00"E, 4 m asl	Malaysia, Pulau Pinang, Pantai Keracut	beach dominated by *Casuarina equisetifolia*	moss, tree branch	Piotr Gąsiorek & Artur Oczkowski
	MY.242	5°27'13"N, 100°11'08"E, 53 m asl	Malaysia, Pulau Pinang, Pantai Keracut	lowland rainforest	moss, rock	Piotr Gąsiorek & Artur Oczkowski
Bryodelphax decoratus sp. nov.	ID.546	1°50'33"S, 120°16'34"E, 800 m asl	Indonesia, Central Sulawesi, Lore Lindu, Bada Lembah	cacao tree plantation	moss, tree	Piotr Gąsiorek & Artur Oczkowski
	ID.548	1°50'33"S, 120°16'34"E, 801 m asl	Indonesia, Central Sulawesi, Lore Lindu, Bada Lembah	cacao tree plantation	moss+lichen, tree	Piotr Gąsiorek & Artur Oczkowski
*Bryodelphax maculatus**	GR.050 (=780)	35°23'23"N, 23°39'36"E, 374 m asl	Greece, Crete ,Vlatos	olive tree plantation	moss, olive tree	Peter Degma
Bryodelphax nigripunctatus sp. nov.**	ES.264 (=716)	39°57'00"N, 3°10'50"E, 160 m asl	Spain, The Balearic Islands, Mallorca, Cap de Formentor, Cala Figuera beach, near the road above	sea shore	moss, rock	Peter Degma
Bryodelphax parvulus	IT.010	45°42'12"N, 13°42'53"E, 1 m asl	Italy, Trieste, Grignano Miramare	urban park	moss, wall	Alicja Witwicka
Bryodelphax sp. nov.	ID.464	1°52'48"S 120°15'48"E, 778 m asl	Indonesia, Central Sulawesi, Lore Lindu, Bada Lembah	cacao tree plantation	moss, tree	Piotr Gąsiorek & Artur Oczkowski
Bryodelphax sp. nov.	ID.846	3°10'52"S, 129°02'58"E, 295 m asl	Indonesia, Ambon, pass between Triana and Jerili/Sawai, Seram Tengah	mountain rainforest	lichen, palm tree	Piotr Gąsiorek & Łukasz Krzywański

* First record for Greece, ** First record of a limno-terrestrial tardigrade for Balearic Islands (see Guil 2002).

Table 2. Processing data for populations of *Bryodelphax* investigated in this study. Types of analyses: LCM – imaging and morphometry in PCM/NCM, SEM – imaging in SEM, DNA – genotyping. Numbers indicate how many specimens were utilised in a given analysis.

Species	Sample code	Analyses		
		LCM	SEM	DNA
Bryodelphax australasiaticus sp. nov.	MY.240	14	10	4
	MY.241	1	–	–
	MY.242	2	–	–
Bryodelphax decoratus sp. nov.	ID.546	9	–	5
	ID.548	3	–	–
Bryodelphax maculatus	GR.050	9	–	6
Bryodelphax nigripunctatus sp. nov.	ES.264	55	30	8
Bryodelphax parvulus	IT.010	8	–	4
Bryodelphax sp. nov.	ID.464	8	–	4
Bryodelphax sp. nov.	ID.846	13	–	4

formed or twisted and their orientations were suitable. Body length was measured from the anterior to the posterior end of the body, excluding the hind legs. The *sp* ratio is the ratio of the length of a given structure to the length of the scapular plate expressed as a percentage (Dastych 1999). The *bs* ratio is the proportion between the maximal body width and the body length in dorsoventrally orientated specimens (Gąsiorek et al. 2018a). Morphometric data were handled using the Echiniscoidea ver. 1.2 template available from the Tardigrada Register, www.tardigrada.net (Michalczyk and Kaczmarek 2013). Ventral plate configuration is given according to Kaczmarek et al. (2012).

Genotyping and phylogenetics

DNA was extracted from individual animals (all examined under a 400× magnification PCM prior to DNA extraction) following a Chelex 100 resin (Bio-Rad) extraction method (Casquet et al. 2012; Stec et al. 2015). Three DNA fragments were sequenced: the small ribosome subunit 18S rRNA (primers 18S_Tar_Ff1 and 18S_Tar_Rr2 from Stec et al. 2017 and Gąsiorek et al. 2017b, PCR programme from Zeller 2010), the large ribosome subunit 28S rRNA (primers 28S_Eutar_F and 28SR0990 from Gąsiorek et al. 2018b and Mironov et al. 2012 and the PCR programme from Mironov et al. 2012) and the internal transcribed spacer ITS-1 (primers ITS1_Echi_F and ITS1_Echi_R from Gąsiorek et al. 2019a, PCR programme from Wełnicz et al. 2011). Some of the less conservative markers, such as ITS-2 and *COI*, are often difficult to amplify for *Bryodelphax*. All fragments were amplified and sequenced according to the protocols described in Stec et al. (2015). Sequences of 18S rRNA and 28S rRNA were aligned using the default settings of MAFFT version 7 (Katoh et al. 2002; Katoh and Toh 2008), with *Echiniscus lineatus* Pilato et al., 2008 and *Echiniscus testudo* (Doyère, 1840) used as the outgroup. The obtained alignments were edited and checked manually in BioEdit v7.2.6.1 (Hall 1999) and then trimmed to 967 bp (18S rRNA) and 754 bp (28S rRNA), respectively. The aligned sequences were concatenated using SequenceMatrix (Vaidya et al. 2011). PartitionFinder version 2.1.1 (Lanfear et al. 2016) with applied Bayesian Information Criterion (BIC) and greedy algorithm (Lanfear et al. 2012) were used to test for the best scheme of partitioning and substitution models for posterior phylogenetic analysis. The analysis was performed solely for MrBayes purposes. The preferred evolution model was GTR+G for both markers (Nei and Kumar 2000), which was finally chosen for further analyses.

ModelFinder (Kalyaanamoorthy et al. 2017) under the Akaike Information Criterion (AIC) and corrected AIC (AICc) was used to find the best substitution models for two predefined partitions (Chernomor et al. 2016). The programme indicated the following models: TVMe+G4 (18S rRNA) and TIM3e+G4 (28S rRNA). Maximum-likelihood (ML) topologies were constructed using IQ-TREE (Nguyen et al. 2015; Trifinopoulos et al. 2016). Strength of support for internal nodes of ML construction was measured using 1000 ultrafast bootstrap replicates (Hoang et al. 2018). Bootstrap (BS) support values ≥ 85% on the final tree were regarded as well supported and those > 70% as moderately supported. Bayesian inference (BI) marginal posterior probabilities were calculated using MrBayes v3.2 (Ronquist and Huelsenbeck 2003). Random starting trees were used and the analysis was run for ten million generations, sampling the Markov chain every 1000 generations. An average standard deviation of split frequencies of < 0.01 was used as a guide to ensure the two independent analyses had converged. The programme Tracer v1.7 (Rambaut et al. 2018) was then used to ensure Markov chains had reached stationarity and to determine the correct 'burn-in' for the analysis which was the first 10% of generations. The Effective Sample Size values were greater than 200 and consensus tree was obtained after summarising the resulting topologies and discarding the burn-in. In the BI consensus tree, clades recovered with posterior probability (PP) between 0.95 and 1 were considered well supported, those with PP between 0.90 and 0.94 were considered moderately supported and those with lower PP were considered unsupported. All final consensus trees were viewed and visualised by FigTree v.1.4.3 (http://tree.bio.ed.ac.uk/software/figtree). MEGA7.0.26 (Kumar et al. 2016) was used for calculation of uncorrected pairwise distances (Srivathsan and Meier 2012).

Data deposition

Raw morphometric data underlying the description of the new species are deposited in the Tardigrada Register under www.tardigrada.net/register/0064.htm (*B. australasiaticus* sp. nov.), www.tardigrada.net/register/0065.htm (*B. decoratus* sp. nov.), www.tardigrada.net/register/0066.htm (*B. nigripunctatus* sp. nov.). Type DNA sequences are deposited in GenBank.

Results

Molecular phylogeny

Bayesian Inference and Maximum Likelihood trees shared identical topology (Fig. 1). Two lineages, each represented by four species, were recovered: the Oriental clade (*B. arenosus* Gąsiorek, 2018, *B. australasiaticus* sp. nov., *B. decoratus* sp. nov. and *Bryodelphax* sp. nov.) and the Western Palaearctic clade (*B. instabilis* Gąsiorek & Degma, 2018, *B. maculatus* Gąsiorek et al., 2017, *B. nigripunctatus* sp. nov. and *B. parvulus* Thulin, 1928).

Descriptions of new species

Systematic account

Phylum: Tardigrada Doyère, 1840
Class: Heterotardigrada Marcus, 1927
Order: Echiniscoidea Richters, 1926
Family: Echiniscidae Thulin, 1928
Genus: *Bryodelphax* Thulin, 1928

Bryodelphax australasiaticus Gąsiorek, Vončina, Degma & Michalczyk, sp. nov.

http://zoobank.org/BE521B67-6769-4EF5-B3C9-56EB43BF2DFE

Figures 2–4, 12, Table 3

B. australis sp. n. in Claxton (2004)

***Locus typicus* and type material.** 5°27'05"N, 100°11'00"E, 4 m a.s.l.; Pantai Keracut, Pulau Penang, Malaysia. Holotype (adult female; slide MY.240.01) and seven paratypes (5 females, 2 juveniles; slides MY.240.01–04) deposited in the Institute of Zoology and Biomedical Research, Jagiellonian University; two paratypes (2 females; slide MY.240.05) deposited in the Department of Zoology, Comenius University in Bratislava; one paratype (1 female; slide MY.240.06) deposited in the Natural History Museum of Denmark, University of Copenhagen; two paratypes (2 females; slide MY.240.07) deposited in the Department of Animal Biology, University of Catania; three paratypes (2 females, one larva; slides MY.241.02, MY.242.02) deposited in the Raffles Museum of Biodiversity Research, National University of Singapore.

Etymology. The name refers to the currently identified geographic range of the new species that encompasses Asia and Australia. Adjective in the nominative singular.

Adults. Body pink, pearly opalescent; eyes absent or not visible after mounting in Hoyer's medium. Primary and secondary clavae small and conical. Cirri *interni* and *externi* with poorly-developed cirrophores. Cirri *A* of typical length for *Bryodelphax*, i.e. reaching around 25% of the total body length. All dorsal plates with barely-discernible intra-cuticular pillars (better visible under a 1000× magnification), the centro-posterior portion of the caudal (terminal) plate has evident, largest pillars (Fig. 2A). Dark epicuticular granules absent (Figs 3; 4A, B), but lateral margins of all dorsal plates and internal margins of facets constituting the scapular plate distinctly thicker and, consequently, darker (Fig. 2A). Pores large and easily detectable (Figs 2A, 3A, B, 4A, B). Pores distributed unevenly, with the largest number present on the antero-central portion of the scapular plate (17–40 pores/100 μm^2, $\bar{x}$ = 29, N = 16, Fig. 4A) and the central portion of the caudal plate (7–43 pores/100 μm^2, $\bar{x}$ = 31, N = 16, Fig. 4B); other plates more variable in terms of pore density, which is always lower than in the aforementioned elements of the armour (0–26 pores/100 μm^2, $\bar{x}$ = 14, N = 16, Fig. 2A). Scapular plate gently faceted by transverse cuticular extensions (Figs 3A, 4A), with deep sutures separating lateral portions from the central faceted part, extending from the base of cirrophore *A* to the posterior margin of the plate (Fig. 2A). Paired plates divided into two roughly equal anterior and posterior parts by a transverse stripe (Figs 2A, 3A, B). Caudal (terminal) plate with poorly developed sutures, not visible under PCM (Fig. 2A), but present and visible under SEM (Figs 3A, B, 4B). Median plate 1 subdivided into anterior narrow portion with dark posterior edge and posterior pentagonal portion with transverse suture (Figs 2A, 3A). Median plate 2 is the largest amongst median plates, with well-developed anterior pentagonal portion and poorly sclerotised posterior portion (Figs 2A, 3A). Median plate 3 with only the anterior portion fully developed, the posterior portion triangular and rounded (Figs 2A, 3A). Supplementary lateral platelets present at the level of median plates (three pairs of platelets on each body side: a pair between the scapular plate and the first pair of the segmental plates, a pair between the paired plates and a pair between the second pair of segmental plates and the caudal plate; Fig. 2A).

Venter with seven rows of faint, greyish plates (VII:4-4-2-4-2-2-1), of which two plates of the first, subcephalic row are located in a more ventrolateral position (Figs 2B, 3C, D, 10). Under SEM, only the central subcephalic and genital plates are visible as true cuticular thickenings, whereas other plates are visible only as darker areas on the cuticular surface (Fig. 3C, D). Leg papillae undetectable under LCM (Fig. 2), but papillae IV visible under SEM (Fig. 3B, C). Both pulvini and pedal plates present, the former developed as thin rectangular stripes in the proximal leg portions (Figs 2A, 3C) and the latter – as large swellings in the central leg portions (Figs 2A, 3C). Pedal plate IV toothless, but with a distinct dark margin (Fig. 2A). External claws spurless, but internal ones with minute spurs positioned close to the claw bases (Figs 2B [insert], 4C).

Juveniles. Body 73–101 μm long in the two found juveniles. Dorsal and ventral plates developed similarly to adults. Scapular plate 12–16 μm long. Claws 3.7–4.8 μm long.

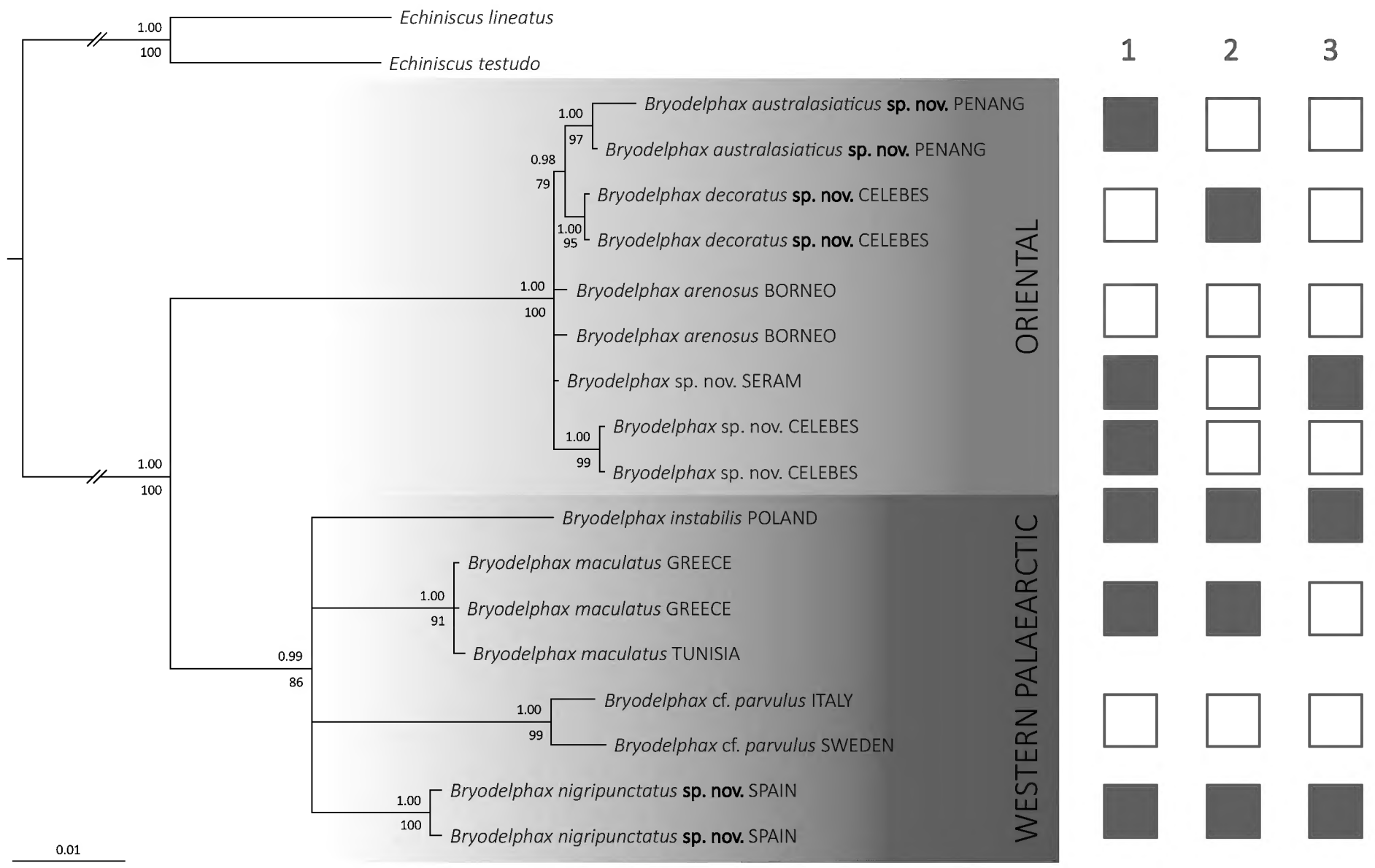

Figure 1. BI and ML concatenated (18S rRNA + 28S rRNA) phylogenetic tree of *Bryodelphax* Thulin, 1928; *Echiniscus* spp. were used as outgroup taxa. Bayesian posterior probability values (≥ 0.90) are given above tree branches, whereas ML bootstrap support values (≥ 70) are below branches. The scale bar represents 0.01 substitutions/site in the Bayesian tree. Trait mapping (blue square – presence, empty square – absence): 1 – ventral plates; 2 – granules on dorsal plates; 3 – males in population.

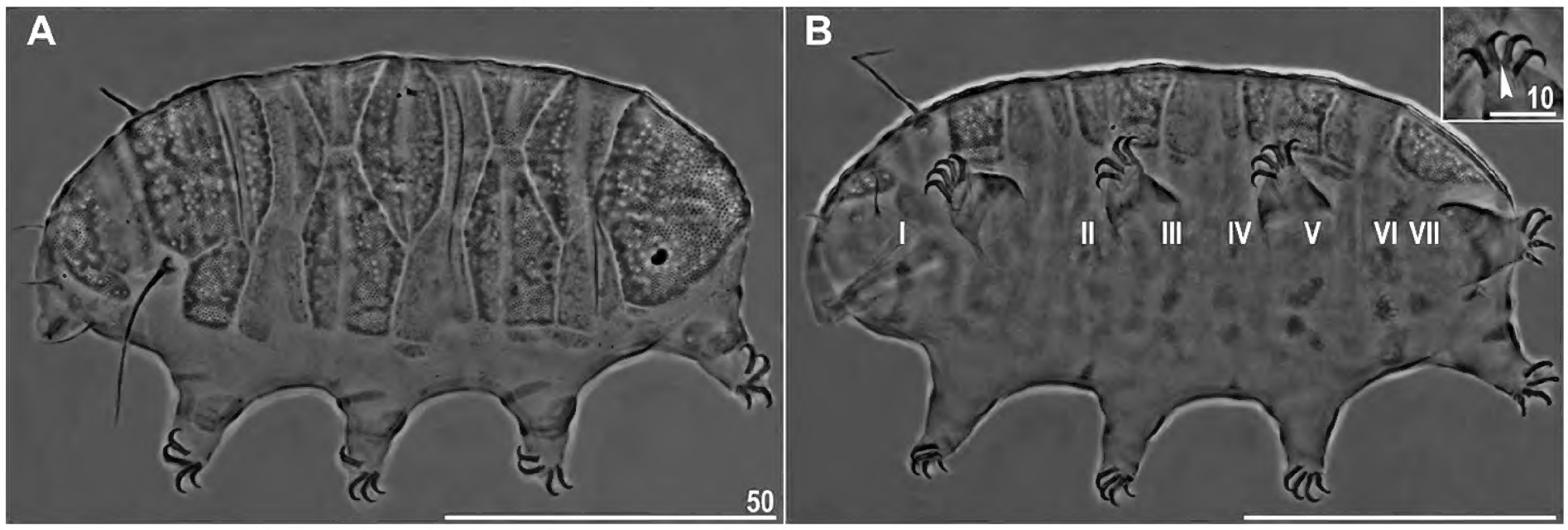

Figure 2. Habitus of adult female of *Bryodelphax australasiaticus* sp. nov. (holotype, PCM): **A** – dorsolateral view; **B** – ventrolateral view (insert with the claws III, arrowhead indicates spur on internal claw). Roman numerals signify ventral plate rows. Scale bars: 50 μm.

Larvae. Body 80 μm long in a single found two-clawed specimen. Dorsal and ventral plates developed similarly to adults. Scapular plate 12.7 μm long. Claws 4.0–4.4 μm long.

Eggs. Up to one egg in exuvia was found.

DNA sequences. Single 18S rRNA haplotype (MT333468), two 28S rRNA haplotypes (MT333460–1) and single ITS-1 haplotype (MT333477).

Phenotypic differential diagnosis. Within the *weglarskae* group, only *B. decoratus* sp. nov., *B. sinensis* and *B. instabilis* have seven plate rows, but *B. olszanowskii* Kaczmarek et al., 2018 exhibits peculiar ventrolateral plates in the subcephalic row and that is why this taxon is also taken into consideration in the differential diagnosis. Adult females of *B. australasiaticus* sp. nov. are differentiated from:

- *B. decoratus* sp. nov., by the ventral plate formula (VII:4-4-2-4-2-2-1 in the new species vs. VII:4-2-

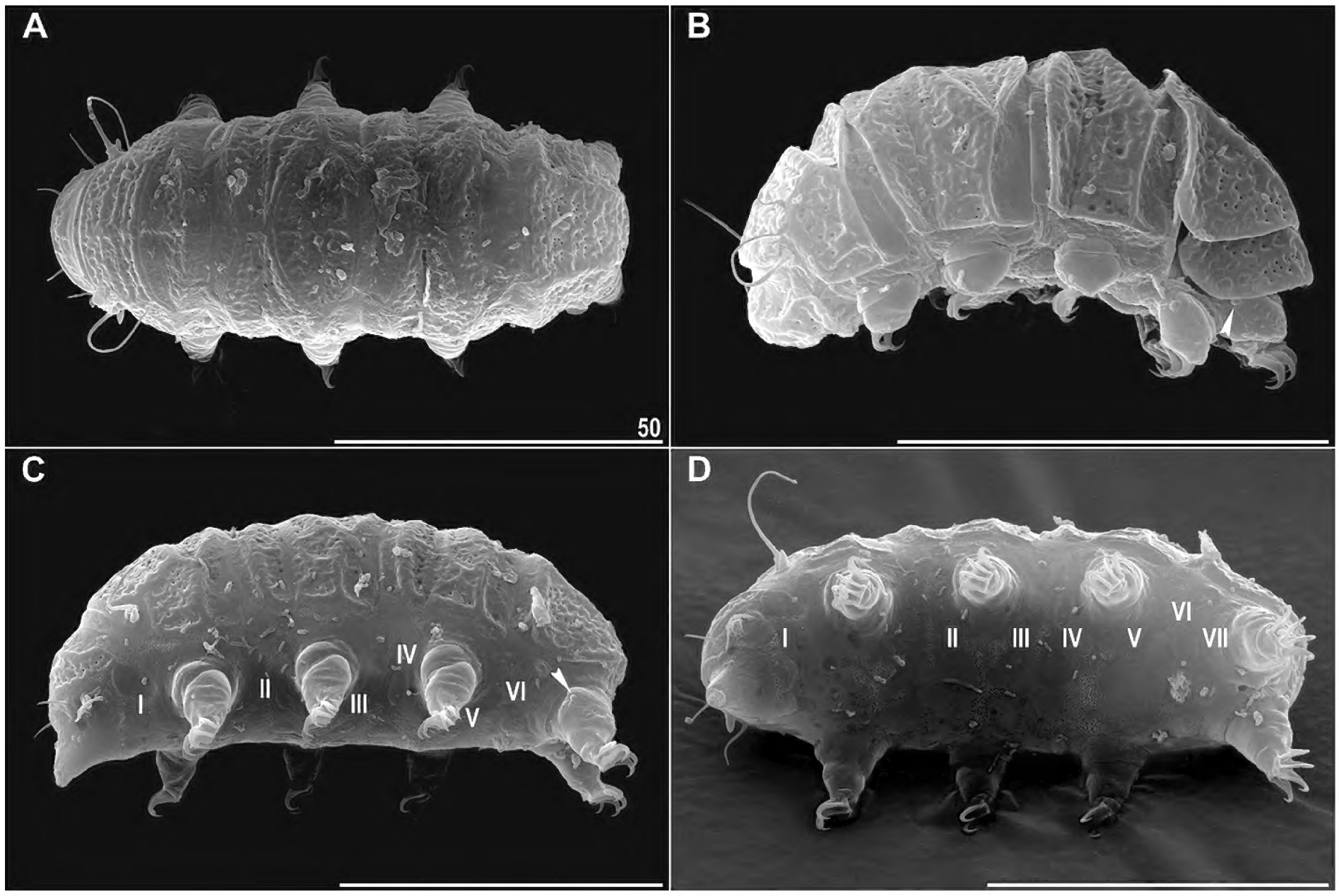

Figure 3. Habitus of adult females of *Bryodelphax australasiaticus* sp. nov. (paratypes, SEM): **A** – dorsal view; **B** – lateral view; **C** – ventrolateral view; **D** – ventral view. Roman numerals signify ventral plate rows and arrowheads indicate papillae on fourth pair of legs. Scale bars: 50 μm.

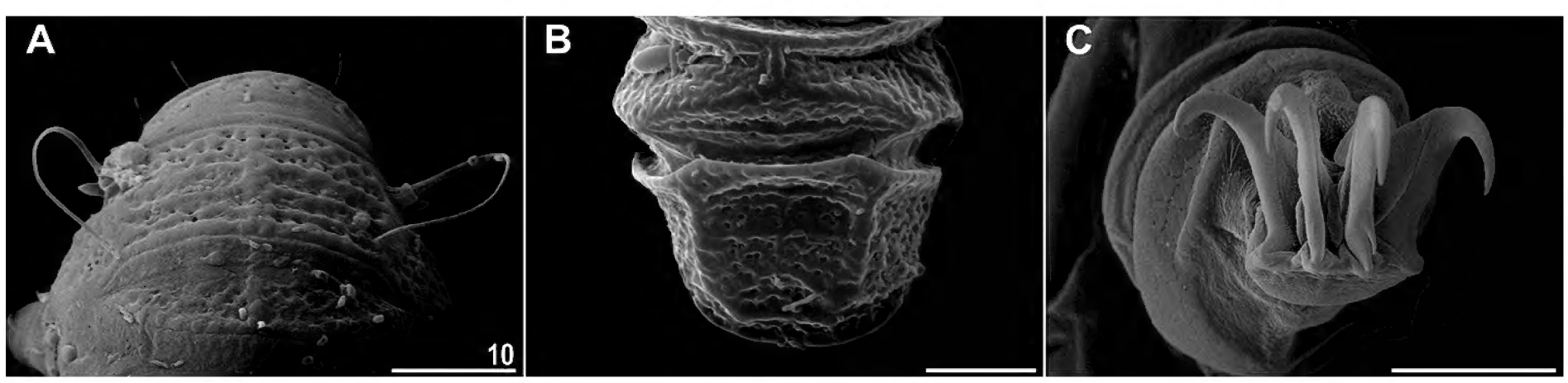

Figure 4. Detailed morphology of *Bryodelphax australasiaticus* sp. nov. (paratypes, SEM): **A** – frontal part of the body, faceting of the scapular plate; **B** – caudal part of the body; **C** – claws III in close-up. Scale bars: 10 μm.

2-4-2-2-1 in *B. decoratus* sp. nov.) and by dorsal plate sculpturing (merged epicuticular ridges surrounding the borders of all dorsal plates in the new species vs. large, dark epicuticular granules in *B. decoratus* sp. nov.);

- *B. sinensis*, known from Caucasus and China (the record from Spitsbergen (Dastych 1985) represents *B. parvuspolaris*), by the ventral plate formula (VII:4-4-2-4-2-2-1 in the new species vs. VII:2-2-2-2-2-2-1 in *B. sinensis*) and the caudal (terminal) plate faceting (invisible under LCM in the new species vs. four facets formed by the raised plate areas between two longitudinal and one transversal sutures in *B. sinensis*);
- *B. instabilis*, currently considered endemic to the Tatras and northern Slovakia, by the ventral plate formula (VII:4-4-2-4-2-2-1 in the new species vs. VII/IX:(2)-(1)-2/4-2-2/4-2-2-2-1 in *B. instabilis*), the presence of dentate collar IV (absent in the new species vs. present in *B. instabilis*), the detectability of papilla IV under LCM (undetectable in the new species vs. detectable in *B. instabilis*) and by the reproductive mode (parthenogenesis in the new species vs. dioecy in *B. instabilis*);
- *B. olszanowskii*, reported from the Antarctic, by the ventral plate formula (VII:4-4-2-4-2-2-1 in the new species vs. VIII:4-1-1-2-2-2-2-2 in *B. olszanowskii*), the presence of dark epicuticular granules (ab-

Table 3. Measurements [in µm] of selected morphological structures of mature females of *Bryodelphax australasiaticus* sp. nov. mounted in Hoyer's medium (**N** – number of specimens/structures measured, **Range** refers to the smallest and the largest structure amongst all measured specimens; **SD** – standard deviation; ***sp*** – the ratio of the length of a given structure to the length of the scapular plate expressed as a percentage).

Character	N	Range						Mean		SD		Holotype	
		µm			*sp*			µm	*sp*	µm	*sp*	µm	*sp*
Body length	16	91	–	119	*584*	–	*737*	108	*667*	7	*41*	111	*666*
Scapular plate length	16	15.2	–	17.9		–		16.2	–	0.8	–	16.6	–
Head appendages lengths													
Cirrus *internus*	15	4.7	–	6.6	*30.2*	–	*42.4*	5.7	*35.4*	0.6	*4.0*	5.6	*33.9*
Cephalic papilla	12	2.3	–	3.3	*13.9*	–	*21.1*	2.9	*18.0*	0.3	*2.3*	2.9	*17.6*
Cirrus *externus*	14	7.4	–	9.4	*47.7*	–	*58.6*	8.4	*52.6*	0.5	*3.3*	9.0	*54.3*
Clava	11	1.8	–	3.1	*10.7*	–	*20.4*	2.3	*14.0*	0.4	*2.8*	1.9	*11.2*
Cirrus *A*	17	23.2	–	28.7	*144.0*	–	*183.6*	25.8	*160.0*	1.6	*11.6*	24.6	*147.7*
Cirrus *A*/Body length ratio	15	21%	–	26%		–		24%	–	1%	–	22%	–
Claw heights													
Claw I	13	4.5	–	5.7	*26.2*	–	*33.9*	5.1	*31.2*	0.4	*2.2*	5.1	*30.4*
Claw II	14	4.3	–	5.5	*26.7*	–	*33.3*	5.0	*30.4*	0.3	*2.3*	5.5	*33.3*
Claw III	15	4.2	–	5.5	*26.5*	–	*34.2*	4.8	*29.6*	0.3	*2.1*	5.0	*30.2*
Claw IV	13	4.9	–	6.2	*30.7*	–	*38.4*	5.4	*33.3*	0.4	*2.7*	5.4	*32.2*

sent in the new species vs. present and accumulated on ventral plates in *B. olszanowskii*) and the detectability of papilla IV under LM (absent in the new species vs. present in *B. olszanowskii*).

Genotypic differential diagnosis: *p*-distances between the new species and the remaining *Bryodelphax* spp., for which DNA sequences are available, were as follows:

- 18S rRNA: from 0.3% (*B. decoratus* sp. nov., MT333469–70) to 3.4% (*B.* cf. *parvulus*, HM193371);
- 28S rRNA from 0.5% (*Bryodelphax* sp. nov. from Celebes, MT333467) to 9.3% (*B.* cf. *parvulus*, MT333466);
- ITS-1: from 2.6% (*B. arenosus*, MT346599–600) to 3.3% (*B. decoratus* sp. nov., MT333478).

Remarks. Two ventrolateral plates were not drawn in Claxton (2004), which is an unpublished PhD dissertation, thus the species described therein are not valid. However, having ascertained that these structures exist in specimens from Australia, the compared populations from both continents appeared identical in terms of morphology.

Bryodelphax decoratus Gąsiorek, Vončina, Degma & Michalczyk, sp. nov.

http://zoobank.org/B009F420-45BF-4B38-B752-E9CE578AB5A5

Figures 5, 6, 12, Table 4

***Locus typicus* and type material.** 1°50'33"S, 120°16'34"E, 800 m a.s.l.; Bada Lembah, Lore Lindu, Celebes (Sulawesi), Indonesia. Holotype (adult female, slide ID.546.15) and three paratypes (females; slide ID.546.12) deposited in the Institute of Zoology and Biomedical Research, Jagiellonian University; three paratypes (females; slide ID.546.13) deposited in the Department of Zoology, Comenius University in Bratislava; three paratypes (females; slide ID.548.11) deposited in the Natural History Museum of Denmark, University of Copenhagen; one paratype (female; slide ID.546.14) deposited in the Department of Animal Biology, University of Catania; one paratype (female; slide ID.546.16) deposited in the Raffles Museum of Biodiversity Research, National University of Singapore.

Etymology. From Latin *decoratus* = beautified, embellished. The name highlights the intricate and beautiful pattern of the dark epicuticular granules. Adjective in the nominative singular.

Adults. Body translucent; eyes absent or not visible after mounting in Hoyer's medium. Primary and secondary clavae minute and conical. Cirri *interni* and *externi* with poorly developed cirrophores. Cirri *A* of typical length for *Bryodelphax*, i.e. reaching around 25% of the total body length. All dorsal plates with well-visible intra-cuticular pillars, the largest pillars present on the scapular, posterior portions of paired segmental and the caudal (terminal) plates (Fig. 5). Dark epicuticular granules present on the dorsum (Figs 5, 6), forming visible transverse lines on the scapular plate, distributed along the margins of all plates, lateral scapular sutures and caudal sutures; additionally, two lines of granules parallel to the lateral margins of paired segmental plates are visible (Figs 5, 6). Pores large and easily detectable (Fig. 5), but their number varies considerably between both specimens and different elements of the armour, with the largest numbers present on the antero-central portion of the scapular plate and median plate 2 (23–48 pores/100 µm^2, $\bar{x}$ = 32 and 23–47 pores/100 µm^2, $\bar{x}$ = 33, respectively; N = 12) and lower numbers on the central portions of the caudal plate and paired segmental plate II (1–38 pores/100 µm^2, $\bar{x}$ = 19 and 10–27 pores/100 µm^2, $\bar{x}$ = 17, respectively; N = 12). Scapular plate with lighter rectangles (pseudofacets) between three or four transverse rows of merged dark epicuticular gran-

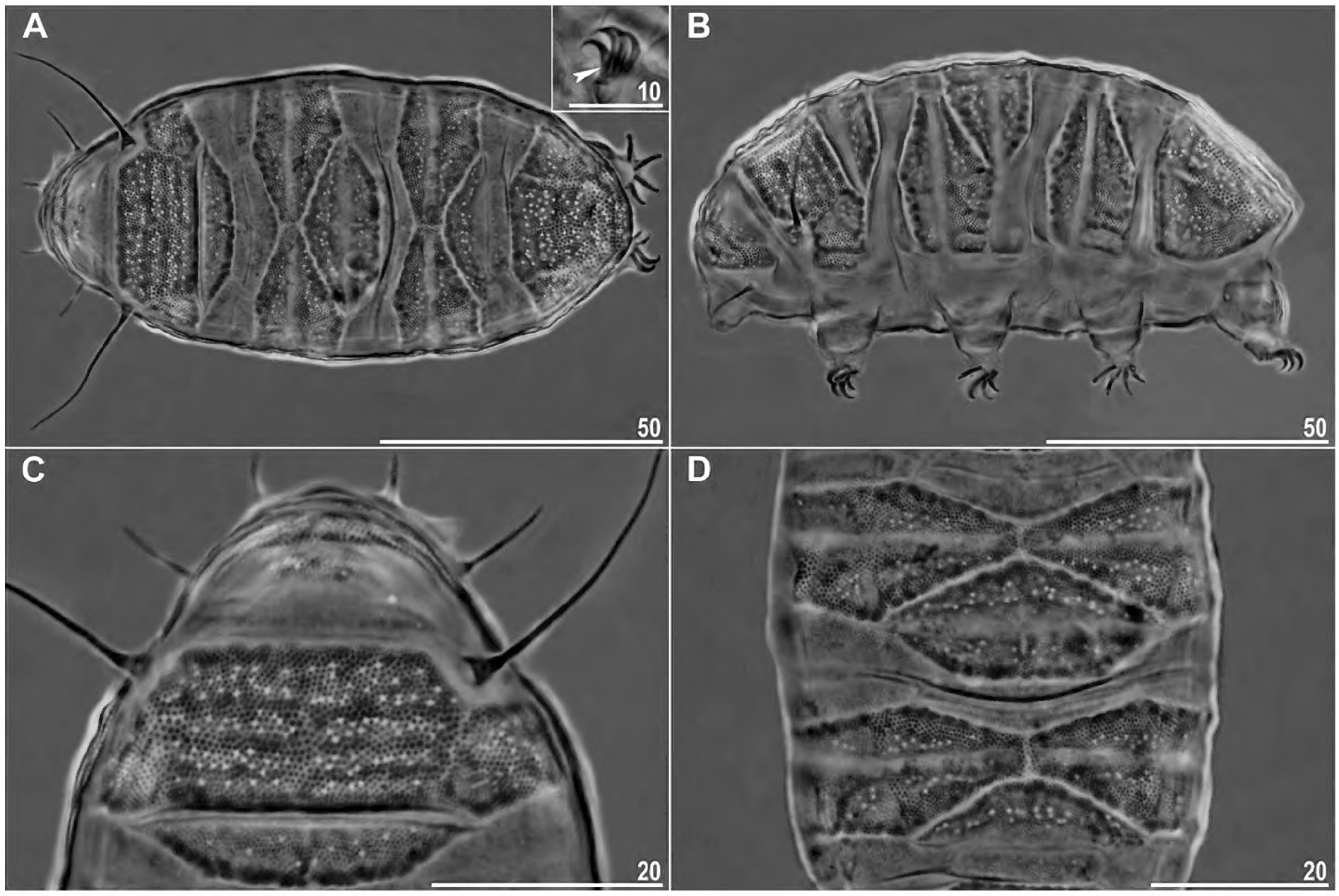

Figure 5. Habitus of adult females of *Bryodelphax decoratus* sp. nov. (PCM): **A** – holotype, dorsal view (insert with the claws I, arrowhead indicates spur on internal claw); **B** – paratype, lateral view; **C** – frontal part of the body; **D** – central part of the body, sculpture of median and paired plates. Scale bars in µm.

ules (Figs 5C, 6). Paired plates divided into two equal anterior and posterior parts by a transverse stripe (Fig. 5D). Caudal (terminal) plate with poorly developed sutures (Fig. 5A). Median plate 1 subdivided into the narrow anterior portion with dark epicuticular granules accumulated at the posterior edge and the posterior, unsculptured pentagonal portion with transverse suture (Fig. 5A, D). Median plate 2 is notably the largest amongst median plates, with well-developed anterior pentagonal portion and weakly-sclerotised posterior portion (Fig. 5A, D). Median plate 3 with the anterior portion fully developed, triangular and a smaller rounded posterior portion (Fig. 5A, D). Supplementary lateral platelets present and detectable at lateral-most margins of the segmental plates (Fig. 5B).

Venter with extremely weakly delineated plates (VII:4-2-2-4-2-2-1), only slightly darker than the surrounding ventral cuticle and without clear, sclerotised margins. Dark epicuticular granules and intra-cuticular pillars absent. Leg papillae undetectable under LCM. Both pulvini and pedal plates absent (Fig. 5B). Dentate collar IV absent. External claws spurless, but internal ones with minute spurs barely divergent from the claw branches (Fig. 5A, insert).

Juveniles. Not found.

Larvae. Not found.

Eggs. Not found.

DNA sequences. Two 18S rRNA haplotypes (MT333469–70) and two 28S rRNA haplotypes (MT333462–3) and single ITS-1 haplotype (MT333478).

Phenotypic differential diagnosis. The new species belongs to the *weglarskae* group and it must be compared with the three species (*B. instabilis*, *B. olszanowskii* and *B. sinensis*) with seven ventral plate rows or with ventrolateral plates in the first row present. Additionally, *B. decoratus* sp. nov. is compared with *B. arenosus*, as the new species can have very dim and barely discernible ventral plates and, in such cases, it resembles *B. arenosus*. Nevertheless, adult females of *B. decoratus* sp. nov. differ specifically from:

- *B. arenosus*, currently considered endemic to Borneo, by body length (99–120 µm in the new species vs. 76–95 µm in *B. arenosus*) and dorsal plate sculpturing (separate granules present on entire dorsum in the new species vs. continuous, thickened ridges present on the lateral portions of plates in *B. arenosus*);
- *B. sinensis*, by the ventral plate formula (VII:4-2-2-4-2-2-1 in the new species vs. VII:2-2-2-2-2-2-1 in *B. sinensis*) and the caudal (terminal) plate faceting (invisible under LCM in the new species vs. four facets formed by the raised plate areas between two longitudinal and one transversal sutures in *B. sinensis*);
- *B. instabilis*, by the ventral plate formula (VII:4-2-2-4-2-2-1 in the new species vs. VII/IX:(2)-(1)-

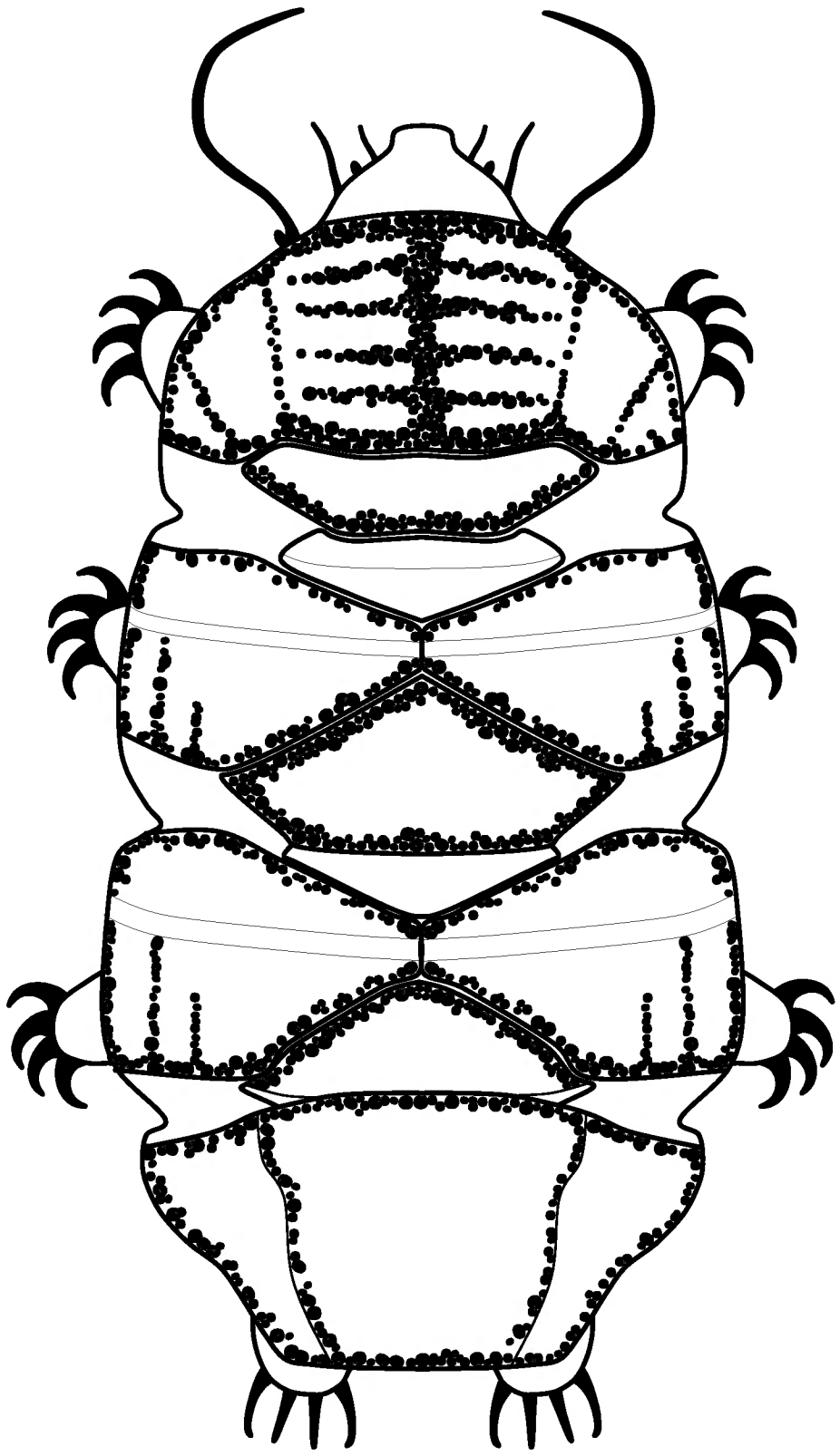

Figure 6. Semi-schematic drawing of the arrangement of epicuticular granules on dorsal armour of *Bryodelphax decoratus* sp. nov.

2/4-2-2/4-2-2-2-1 in *B. instabilis*), the absence of dentate collar IV (present in *B. instabilis*), the detectability of papilla IV under LCM (undetectable in the new species vs. detectable in *B. instabilis*) and by the reproductive mode (parthenogenesis in the new species vs. dioecy in *B. instabilis*);

- *B. olszanowskii*, by the ventral plate formula (VII:4-2-2-4-2-2-1 in the new species vs. VIII:4-1-1-2-2-2-2-2 in *B. olszanowskii*), the presence of dark epicuticular granules on the dorsum (absent in *B. olszanowskii*) and by the detectability of papilla IV under LCM (undetectable in the new species vs. detectable in *B. olszanowskii*).

Genotypic differential diagnosis: *p*-distances between the new species and the remaining *Bryodelphax* spp., for which DNA sequences are available, were as follows:

- 18S rRNA: from 0.3% (*B. australasiaticus* sp. nov., MT333468) to 3.1% (*B.* cf. *parvulus*, HM193371);
- 28S rRNA from 0.3% (*B. australasiaticus* sp. nov. and *Bryodelphax* sp. nov. from Celebes, MT333460, MT333461, and MT333467, respectively) to 9.5% (*B.* cf. *parvulus*, MT333466);
- ITS-1: from 3.1% (*B. arenosus*, MT346599) to 23.4% (*B. maculatus*, MT333479).

Bryodelphax nigripunctatus Degma, Gąsiorek, Vončina & Michalczyk, sp. nov.

http://zoobank.org/48DA4500-2806-491E-8AD8-D2C830AF39F4

Figures 7–12, Tables 5–6

***Locus typicus* and type material.** 39°57'00"N, 3°10'50"E, 160 m a.s.l.; near the road above Cala Figuera beach, Cap de Formentor, NE Mallorca, the Balearic Islands, Spain. Holotype (adult female; together with one male paratype in slide 716/45), allotype (adult male; slide 716/9) and 30 paratypes (9 females, 14 males, 3 specimens of unknown sex, 2 juveniles and 2 larvae; slides 716/1–5, 10, 13, 17–20, 25, 27–29, 32–34, 41, 45, 47–48, 50–51) deposited in the Department of Zoology, Comenius University

Table 4. Measurements [in µm] of selected morphological structures of mature females of *Bryodelphax decoratus* sp. nov. mounted in Hoyer's medium (**N** – number of specimens/structures measured, **Range** refers to the smallest and the largest structure amongst all measured specimens; **SD** – standard deviation; ***sp*** – the ratio of the length of a given structure to the length of the scapular plate expressed as a percentage).

Character	N	Range						Mean		SD		Holotype	
		µm			*sp*			µm	*sp*	µm	*sp*	µm	*sp*
Body length	13	99	–	120	*595*	–	*694*	107	*633*	6	*32*	104	*640*
Scapular plate length	13	16.1	–	18.2		–		16.9	–	0.7	–	16.2	–
Head appendages lengths													
Cirrus *internus*	13	4.6	–	7.0	*28.5*	–	*42.3*	6.0	*35.7*	0.8	*4.2*	5.4	*33.0*
Cephalic papilla	11	2.5	–	3.5	*15.4*	–	*20.5*	3.1	*18.4*	0.4	*1.7*	3.3	*20.5*
Cirrus *externus*	11	8.1	–	12.2	*50.2*	–	*70.6*	9.6	*57.2*	1.3	*7.3*	9.0	*55.4*
Clava	9	2.2	–	3.0	*13.1*	–	*18.4*	2.6	*15.3*	0.2	*1.8*	?	*?*
Cirrus *A*	12	24.1	–	27.7	*137.6*	–	*169.5*	25.9	*153.4*	1.2	*9.5*	27.4	*169.3*
Cirrus *A*/Body length ratio	12	22%	–	28%		–		24%	–	2%	–	26%	–
Claw heights													
Claw I	11	5.0	–	6.2	*29.8*	–	*35.1*	5.5	*32.5*	0.4	*1.9*	?	*?*
Claw II	11	4.4	–	5.5	*26.5*	–	*33.3*	5.1	*30.2*	0.4	*2.0*	4.8	*29.8*
Claw III	13	4.6	–	5.7	*28.1*	–	*34.1*	5.2	*30.8*	0.4	*1.7*	4.9	*30.1*
Claw IV	13	5.2	–	6.4	*32.2*	–	*39.2*	5.8	*34.6*	0.4	*2.4*	5.2	*32.2*

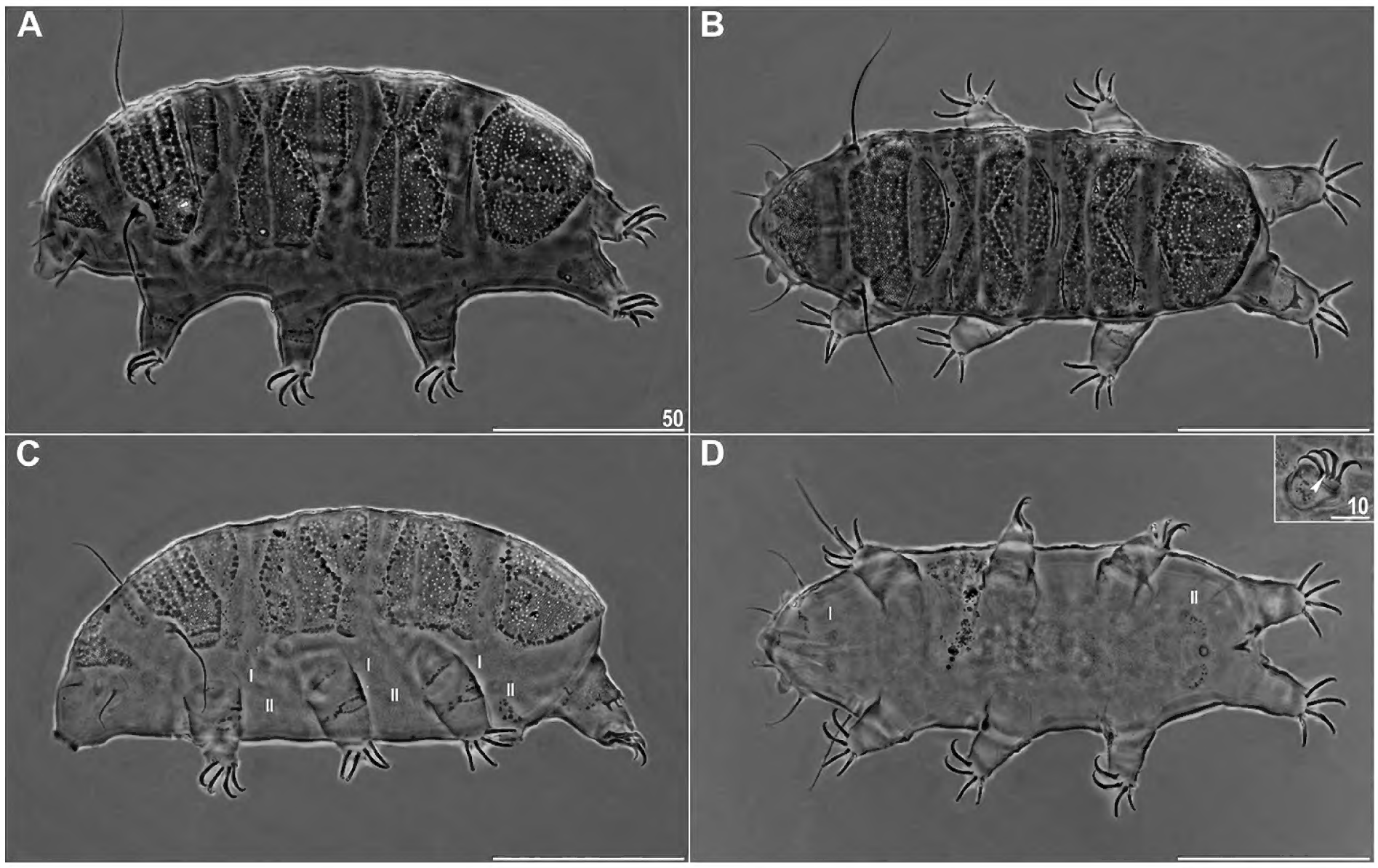

Figure 7. Habitus of adults of *Bryodelphax nigripunctatus* sp. nov. (PCM): **A** – female (holotype, dorsolateral view); **B** – male (allotype, dorsal view); **C** – female (paratype, lateral view; Roman numerals signify epicuticular belts of granules on legs); **D** – male (allotype, ventral view, Roman numerals point out reduced ventral armature; insert with the claws II, arrowhead indicates spur on internal claw). Scale bars: 50 μm.

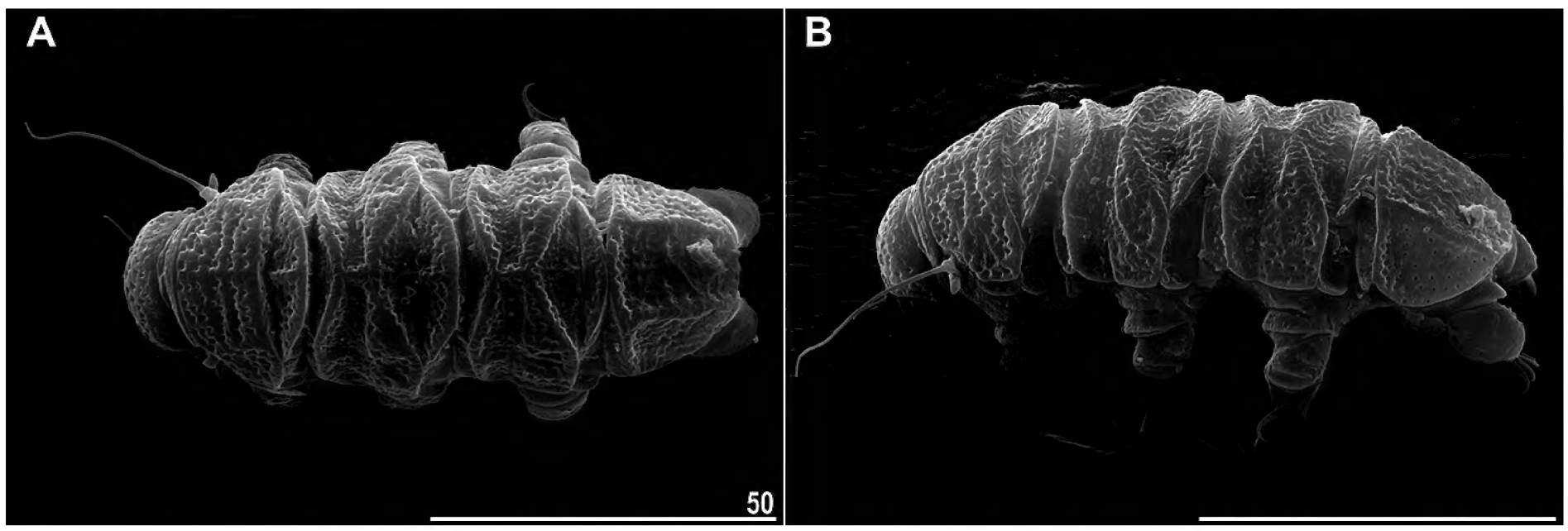

Figure 8. Habitus of adult male of *Bryodelphax nigripunctatus* sp. nov. (paratype, SEM): **A** – dorsal view; **B** – lateral view. Scale bars: 50 μm.

in Bratislava; 13 paratypes (6 females, 6 males and one specimen of unknown sex; slides 716/26, 38, 40, 42–44, 46, 49) deposited in the Institute of Zoology and Biomedical Research, Jagiellonian University; 9 paratypes (4 females and 5 males; slides 716/6–8, 11–12, 22–24, 35) deposited in the Natural History Museum of Denmark, University of Copenhagen; 9 paratypes (4 females and 5 males; slides 716/14–16, 21, 31, 36–37) deposited in the Department of Animal Biology, University of Catania. Single paratype (male) mounted on a SEM stub (14.19) deposited in the Institute of Zoology and Biomedical Research, Jagiellonian University. Eight specimens used for DNA extraction. *Bryodelphax nigripunctatus* sp. nov. was not accompanied by other species in the sample.

Etymology. From Latin *niger* = black + *punctum* = dot, spot. The name underlines evident epicuticular granules appearing dark in PCM and contrasting with other elements of dorsal sculpture. Adjective in the nominative singular.

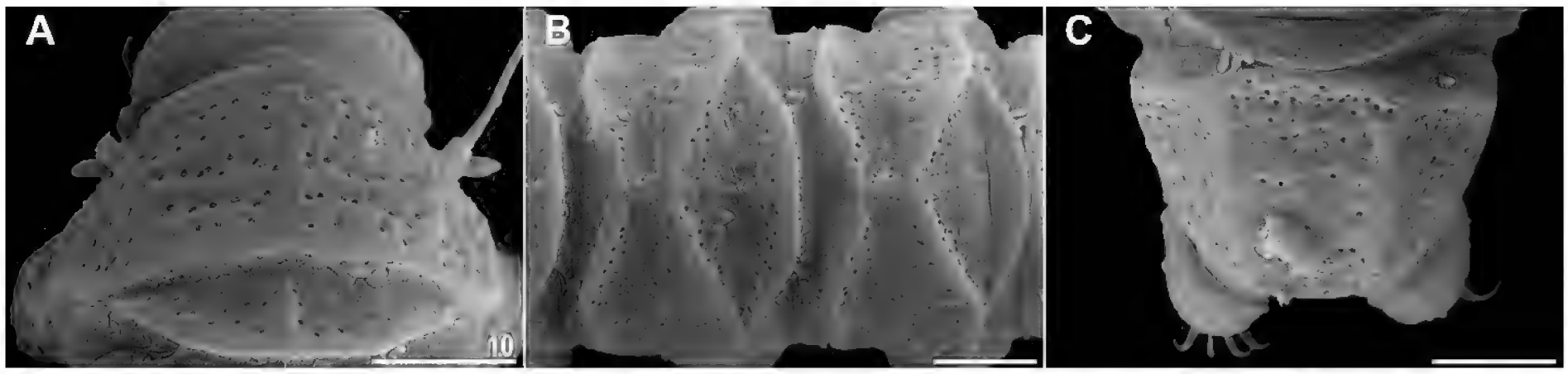

Figure 9. Detailed morphology of *Bryodelphax nigripunctatus* sp. nov. (paratype, SEM): **A** – frontal part of the body; **B** – central part of the body; **C** – caudal part of the body. Scale bars: 10 µm.

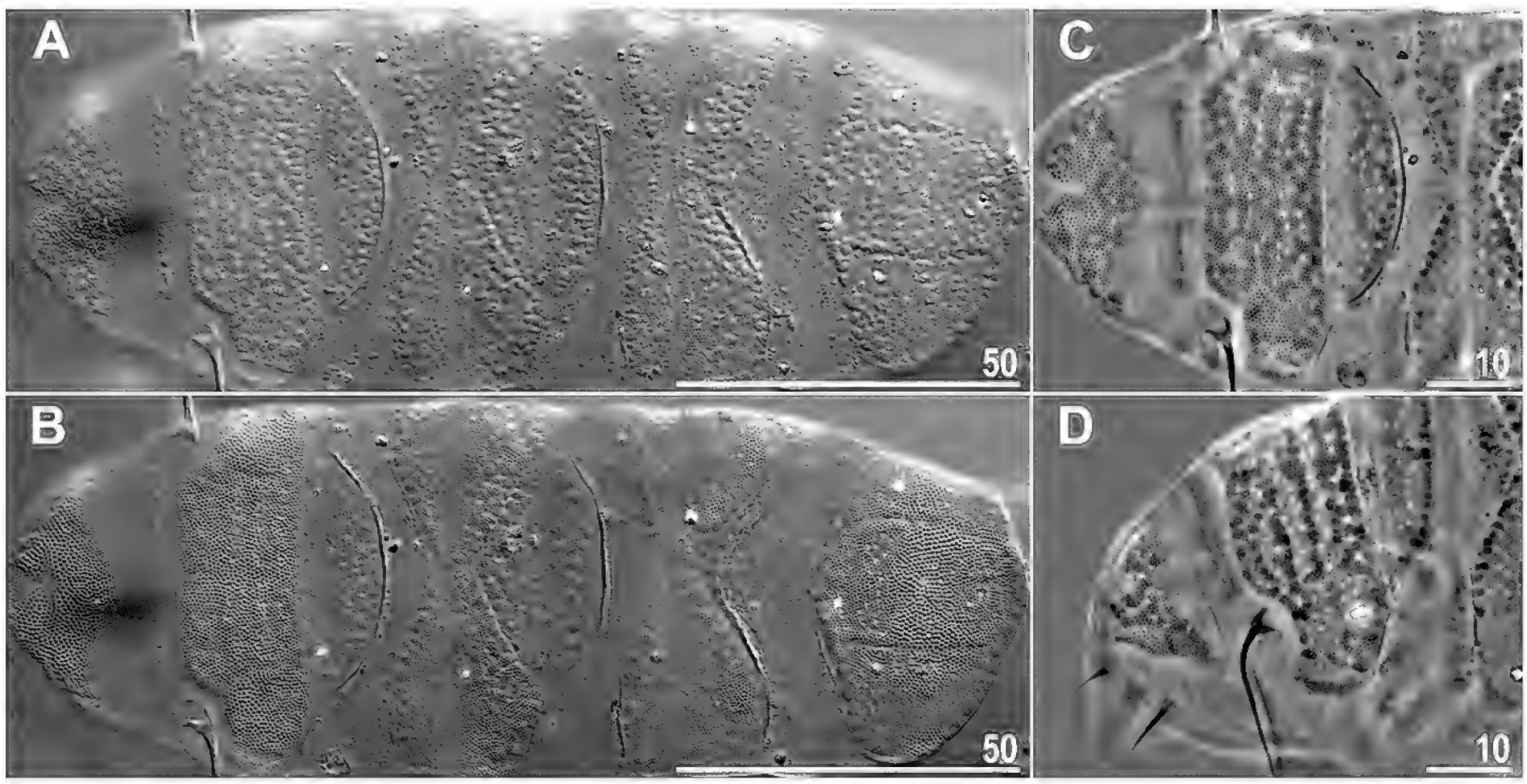

Figure 10. Details of cuticular sculpturing of *Bryodelphax nigripunctatus* sp. nov.: **A** – microscope focused on the epicuticular granules (allotype, NCM); **B** – microscope focused on the intracuticular pillars (allotype, NCM); **C** – frontal part of the body (allotype, PCM); **D** – frontal part of the body (holotype, PCM). Scale bars in µm.

Adults. Body translucent without distinct colour and usually stout in females and more slender in males (Figs 7, 8), *bs* = 43.0–49.2% ($\bar{x}$ = 45.6%, N = 8) in females and 37.5–44.7% ($\bar{x}$ = 39.8%, N = 10) in males. Eyes absent or not visible after mounting in Hoyer's medium. Cephalic papillae and clavae elliptical with rounded apex. Cephalic papilla is relatively broader in males than in females. Both cephalic papillae and primary clavae relatively longer in males than in females (Figs 7A, B, 10C, D; compare the *sp* of the cephalic papilla and clava in Tables 5, 6). Cirri *interni* always shorter than cirri *externi* and both with poorly-developed cirrophores. Cirri *A* reach around 1/5–1/4 of the total body length (Tables 5, 6). Unappendaged. Cuticular sculpture consists of large epicuticular granules, true pores and intra-cuticular pillars (Fig. 10). In PCM, these structures appear, respectively, as conspicuous large dark spots, smaller bright spots and fine dark and dense punctuation (pseudogranulation). Epicuticular granules of irregular shape and size (up to ca. 1.6 µm) are merged together (as visible in SEM, Figs 8–10) and arranged in rows along the margins of all plates, although they are least visible or absent in posterior median plate 1 and posterior median plate 2. Moreover, in the cervical (neck) plate, the row or a double row of granules is also present along its transverse axis. Granules in rows appear as dark spots in PCM (Fig. 7A–C). Similar rows of granules cover also folds which create the faceting of the scapular and caudal plate: median and two lateral longitudinal folds (at the level of cirrophores *A*) together with 3–4 posterior transverse folds on the scapular plate and two longitudinal folds dividing the caudal plate into three parallel portions (Figs 7A, B, 8, 9A, C). Finally, short longitudinal rows of granules divide both paired segmental plates and posterior portions of anterior m1–2 plates into left and right portions (Figs 7A, B, 8, 9B). Scattered granules also irregularly cover the surface of the cephalic, paired, caudal, anterior m1–2 and anterior parts of scapular plates (Figs 7A, B, 8, 9, 10A). Round, focusable pores (0.3–0.4 µm in diameter) are unequally distributed on dorsal plates in spaces between

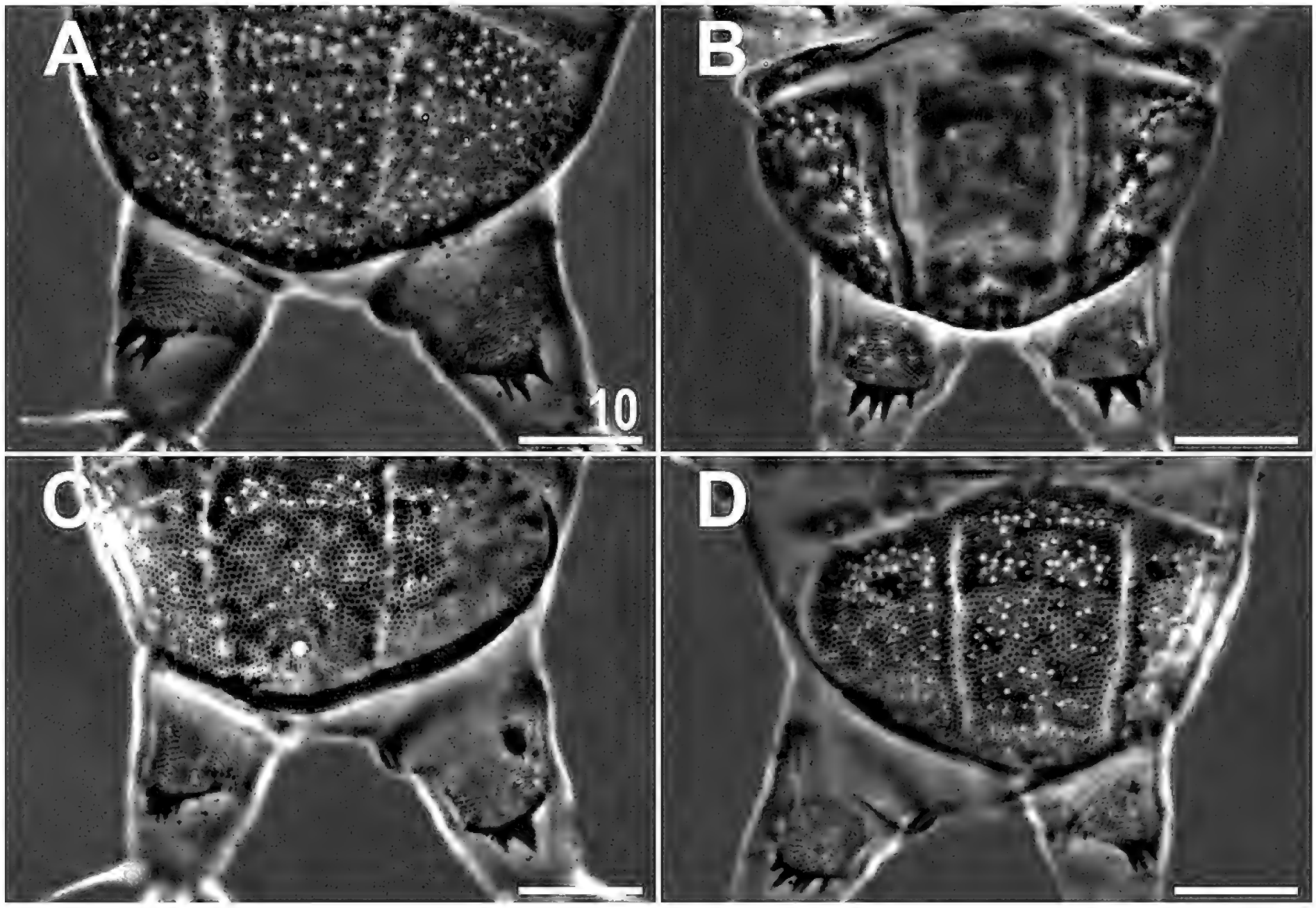

Figure 11. Variability of the dentate collar IV in *Bryodelphax nigripunctatus* sp. nov. (paratypes, PCM). Scale bars: 10 μm.

the scattered granules, on pedal plates IV and between transverse rows of granules in the scapular plate, but they are absent on the rows of granules (Figs 7C, 8, 9A–C, 10B). The density of pores varies between the sexes and elements of armour, with the largest pores present on the segmental plate II, anterior m2 and the scapular plate (21–40 pores/100 μm^2, $\bar{x}$ = 29, 14–28 pores/100 μm^2, $\bar{x}$ = 22 and 18–31pores/100 μm^2, $\bar{x}$ = 26, respectively, N = 15 in females and 7–35 pores/100 μm^2, $\bar{x}$ = 29, 0–34 pores/100 μm^2, $\bar{x}$ = 25 and 11–33 pores/100 μm^2, $\bar{x}$ = 25, respectively; N = 15 in males) and lowest density on caudal plate (16–27 pores/100 μm^2, $\bar{x}$ = 22 in females and 7–28 pores/100 μm^2, $\bar{x}$ = 20 in males; N = 15). On the scapular plate (in the area delimited with lateral longitudinal rows of granules), lines of pores tend to alternate with transverse rows of granules (Figs 7A–C, 8A, 9A, 10A, B). Regularly distributed round intra-cuticular pillars (0.1–0.2 μm in diameter) reinforce the entire cuticle (also under the granules), but they are well-visible only in the cephalic, scapular, both paired segmental, caudal, anterior median 1 and anterior median 2 plates (Fig. 10B), as well as on pedal plates IV. On the remaining cuticle, they are weakly (venter) or scarcely (legs) detectable.

Cephalic plate with an anterior chalice-like incision. Each segmental and median plate consists of the anterior and the posterior portion separated each from other with a transverse bright poreless stripe in PCM. Therefore, paired segmental plates are subdivided into the narrower anterior (ca. 1/3–2/5 of the plate length) and the wider posterior portions, trapezoidal anterior median plate 1 is subdivided just behind its anterior margin, pentagonal anterior m2 (the largest amongst the median plates) is divided at approximately equally-long portions, triangular anterior portion of median plate 3 is ca. two times as long (along median body axis) as the posterior one with rounded posterior margin (dividing transverse line of anterior median plates 2–3 correspond with posterior corners of paired segmental plates). Pentagonal posterior median plates 1–2 subdivided at portions of about same lengths. On each body side, the first two pairs of supplementary lateral platelets are connected with anterior and posterior median plates 1–2 and the third pair is connected with the posterior portion of m3 and with the anterior edge of caudal plate. Anterior platelets of each pair have very distinctly-thickened lateral (lower) margins (Figs 7A, B, 8, 9).

Venter with transverse rows of weakly-developed plates unevenly sculptured with epicuticular granules similar to those on the dorsal plates, but a bit smaller. There are three rows of ventral plates in females (the plate formula III:2-2-1) and two rows in males (II:2-2) (Fig. 7D). The outer surface of legs with a narrow well-visible proximal pulvinus and a wide weak distal pedal plate placed in the central part of the leg. A single row of small epicuticular granules (similar to those on ventral plates) on the distal edge of pulvini in legs I–III (rarely, the second row also on their proximal

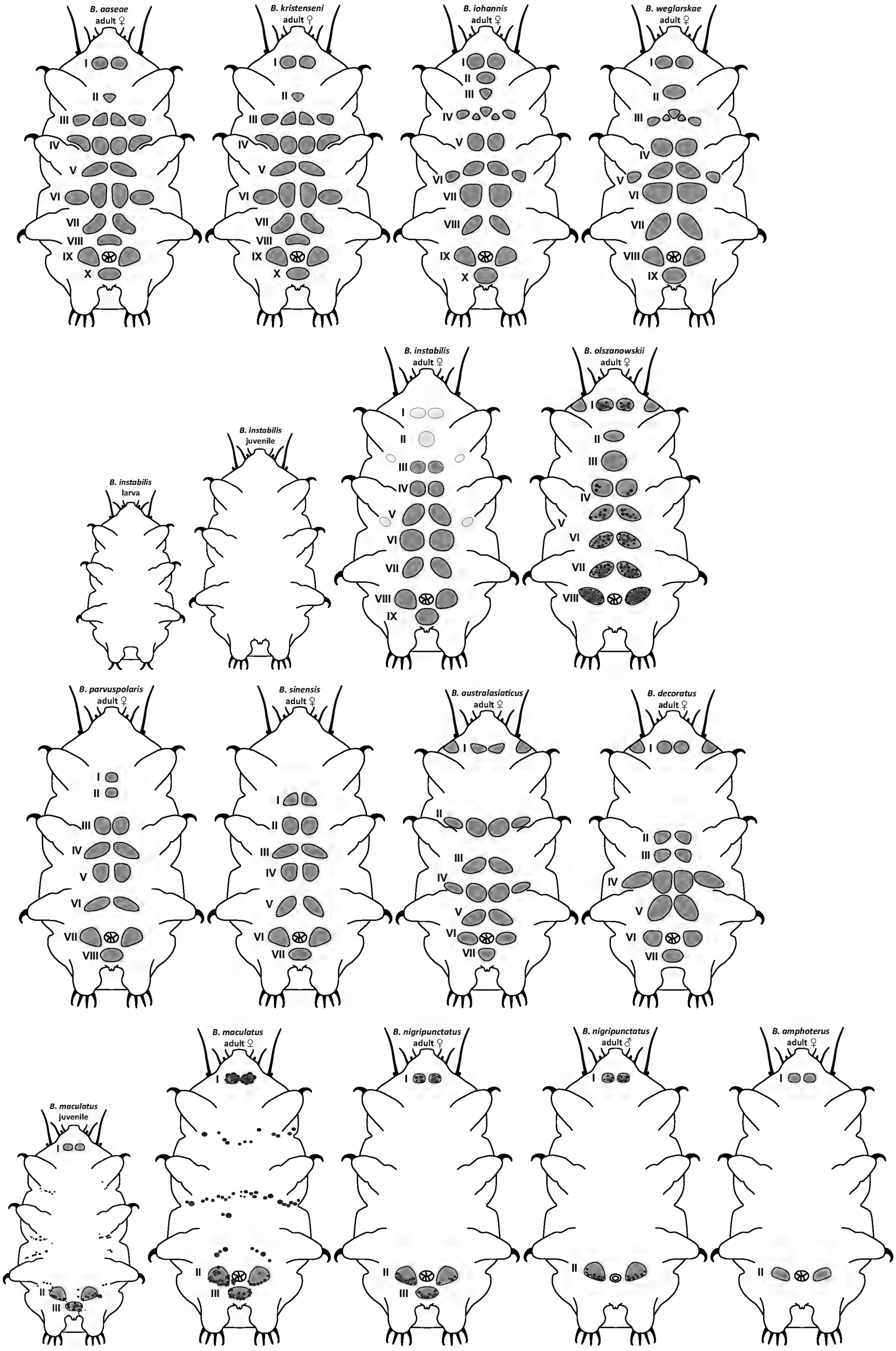

Figure 12. Schematic arrangement of the ventral plates in all members of the *weglarskae* group (species are arranged in order of the increasing reduction of the ventral armature). Known cases of ontogenetic variability and sexual dimorphism are depicted. Following species taken from Kaczmarek et al. (2012): *B. aaseae*, *B. iohannis*, *B. parvuspolaris*, *B. sinensis* and *B. weglarskae*; Gąsiorek et al. (2017a): *B. maculatus*; Gąsiorek & Degma (2018): *B. instabilis*.

Table 5. Measurements [in µm] of selected morphological structures of mature females of *Bryodelphax nigripunctatus* sp. nov. mounted in Hoyer's medium (**N** – number of specimens/structures measured, **Range** refers to the smallest and the largest structure amongst all measured specimens; **SD** – standard deviation; ***sp*** – the ratio of the length of a given structure to the length of the scapular plate expressed as a percentage).

Character	N	Range						Mean		SD		Holotype	
		µm			*sp*			µm	*sp*	µm	*sp*	µm	*sp*
Body length	15	114	–	144	*562*	–	*689*	126	*645*	9	*38*	131	*657*
Scapular plate length	15	18.0	–	21.7		–		19.6	–	1.1	–	19.9	–
Head appendages lengths													
Cirrus *internus*	11	6.1	–	8.9	*32.9*	–	*42.8*	7.3	*37.4*	0.8	*3.3*	7.5	*37.4*
Cephalic papilla	14	2.6	–	3.7	*12.6*	–	*19.7*	3.1	*15.9*	0.4	*1.9*	3.3	*16.5*
Cirrus *externus*	12	10.2	–	12.8	*54.1*	–	*66.9*	11.8	*60.1*	0.7	*4.4*	12.2	*61.4*
Clava	10	2.7	–	3.1	*12.3*	–	*16.9*	2.9	*14.8*	0.1	*1.3*	3.0	*15.0*
Cirrus *A*	15	24.8	–	31.0	*120.7*	–	*163.7*	28.0	*143.6*	1.6	*11.0*	26.3	*132.4*
Cirrus *A*/Body length ratio	15	20%	–	25%		–		22%	–	2%	–	20%	–
Body appendages lengths													
Papilla on leg IV length	8	1.4	–	2.3	*7.2*	–	*12.5*	1.8	*9.5*	0.3	*2.0*	1.5	*7.6*
Number of teeth on the collar	10	2	–	5		–		3.3	–	0.9	–	2	–
Claw heights													
Claw I	12	7.0	–	8.3	*35.1*	–	*44.4*	7.8	*39.8*	0.5	*3.1*	7.2	*36.0*
Claw II	9	7.0	–	8.8	*36.1*	–	*44.3*	7.6	*39.6*	0.5	*2.8*	7.7	*38.8*
Claw III	13	6.7	–	8.3	*36.1*	–	*46.2*	7.6	*39.3*	0.5	*3.1*	7.6	*38.1*
Claw IV	9	7.4	–	8.9	*38.1*	–	*48.0*	8.4	*43.0*	0.5	*3.5*	?	*?*

Table 6. Measurements [in µm] of selected morphological structures of mature males of *Bryodelphax nigripunctatus* sp. nov. mounted in Hoyer's medium (**N** – number of specimens/structures measured, **Range** refers to the smallest and the largest structure amongst all measured specimens; **SD** – standard deviation; ***sp*** – the ratio of the length of a given structure to the length of the scapular plate expressed as a percentage).

Character	N	Range						Mean		SD		Allotype	
		µm			*sp*			µm	*sp*	µm	*sp*	µm	*sp*
Body length	15	106	–	134	*618*	–	*725*	123	*685*	8	*30*	130	*704*
Scapular plate length	15	16.1	–	19.5		–		17.9	–	1.1	–	18.5	–
Head appendages lengths													
Cirrus *internus*	13	6.3	–	9.9	*35.8*	–	*51.7*	7.7	*42.8*	1.0	*4.6*	8.5	*46.0*
Cephalic papilla	14	3.1	–	5.6	*19.0*	–	*32.0*	4.6	*25.5*	0.8	*3.9*	5.2	*28.1*
Cirrus *externus*	13	12.3	–	15.9	*70.6*	–	*85.8*	14.2	*78.6*	1.0	*4.3*	13.9	*75.4*
Clava	11	2.8	–	4.7	*17.6*	–	*24.2*	3.8	*21.2*	0.5	*1.9*	4.1	*21.9*
Cirrus *A*	15	26.8	–	32.6	*141.3*	–	*187.3*	29.3	*163.8*	1.9	*11.4*	30.2	*163.4*
Cirrus *A*/Body length ratio	15	21%	–	26%		–		24%	–	2%	–	23%	–
Body appendages lengths													
Papilla on leg IV length	8	1.7	–	2.4	*9.7*	–	*12.8*	2.0	*11.4*	0.3	*1.0*	2.0	*10.9*
Number of teeth on the collar	12	3	–	5		–		3.9	–	1.0	–	5	–
Claw heights													
Claw I	11	7.3	–	8.7	*37.6*	–	*50.3*	8.1	*45.1*	0.5	*3.4*	8.3	*44.8*
Claw II	10	7.1	–	8.8	*41.2*	–	*48.5*	8.0	*44.7*	0.5	*2.5*	8.8	*47.9*
Claw III	14	7.0	–	9.2	*38.5*	–	*49.5*	8.0	*44.7*	0.6	*3.3*	9.0	*48.6*
Claw IV	9	7.8	–	9.4	*43.6*	–	*52.6*	8.7	*48.3*	0.6	*2.8*	?	*?*

edge). Pedal plates I–III sculptured usually with three (sometimes with more) transverse rows of epicuticular granules, which can be either shortened or connected at their ends (Figs 7A–C, 8B). The pedal plate IV sculptured with distinct intra-cuticular pillars and scattered pores and distally hemmed with dentate collar. The collar with sharp teeth, always longer than the width of their bases and with the distance between teeth similar to their basal widths, although some pairs of teeth can be merged (Fig. 11). Papilla or spine on legs I–III absent, papilla on legs IV well developed. Claws slender, claws IV always slightly longer than claws I–III. External claws smooth, internal ones with a small spur pointing downwards and placed very close to the claw bases (Figs 7A–C, 7D, insert).

Juveniles. In appearance as adults, but smaller (111–112 µm) and with ventral plates just marked with rows of granules. Selected measurements of a shorter specimen: cephalic papilla 3.1 µm, scapular plate 14.9 µm long, claws I–III 5.1–5.6 and claws IV 6.5 µm long.

Larvae. 83–85 µm long. Dorsal plates (especially median ones) mostly with poorly-delineated margins, supplementary lateral platelets absent. Epicuticular granules less numerous than in adults, concentrated mainly on posterior margins of the cephalic, scapular, both paired and caudal plates. Cuticular pores less numerous than in adults, but intracuticular pillars, stripes of granules on the outer surface of legs, papilla on legs IV and dentate collar IV well developed. Ventral plates not visible

in laterally orientated larvae. Claws with spurs formed as in adults. Some measurements of shorter specimen: cephalic papilla 2.5 μm, claws II–III 4.6– 5.3 and claws IV 6.4 μm long.

Eggs. Not found.

DNA sequences. Two 18S rRNA haplotypes (MT333472–3), single 28S rRNA haplotype (MT333465).

Phenotypic differential diagnosis. Having ventral plates, *Bryodelphax nigripunctatus* sp. nov. belongs to the *weglarskae* group. Within the group, only *B. amphoterus* and *B. maculatus* have a reduced number of ventral plate rows to two or three, as in the new species. Consecutively, *B. nigripunctatus* sp. nov. differs from:

- *B. amphoterus*, known from Croatia (Istria) and Greece (Crete) (McInnes 1994), by: the mode of reproduction (dioecy in the new species vs. parthenogenesis in *B. amphoterus*), the presence of lateral supplementary platelets (absent in *B. amphoterus*), the presence of epicuticular granules on dorsal and ventral plates (absent in *B. amphoterus*), a different number of ventral plate rows in females (ventral plate formula III:2-2-1 in females of the new species vs. II:2-2 in *B. amphoterus*) and by the lack of spurs on external claws (extremely small spur very difficult to observe just near the base in *B. amphoterus*);
- *B. maculatus*, known from Tunisia and Greece, by: the mode of reproduction (dioecy in the new species vs. parthenogenesis in *B. maculatus*), large contrasting granules on dorsal plates (granules not contrasting and clearly visible only in SEM in *B. maculatus*), the absence of patches or transverse stripes of epicuticular granules on ventral cuticle between legs (present in *B. maculatus*), a smaller maximal pore density (21–40 pores per 100 μm^2 in segmental II plate in the new species females vs. 48–61 pores per 100 μm^2 in the same plate in *B. maculatus*), a relatively longer internal peribuccal cirrus (*sp* is 33–43% in females of the new species vs. 21–30% in *B. maculatus*) and by relatively longer claws II–IV (*sp* for claws II is 36–44%, for claws III 36–46%, for claws IV 38–48% in females of the new species vs. 29–36%, 30–34% and 32–38%, respectively in *B. maculatus*).

Genotypic differential diagnosis: *p*-distances between the new species and the remaining *Bryodelphax* spp., for which DNA sequences are available, were as follows:

- 18S rRNA: from 0.4% (*B. maculatus*, KY609137 and MT333471) to 2.9% (*B. australasiaticus* sp. nov., MT333468);
- 28S rRNA from 4.2% (*B. instabilis*, MH414965) to 8.1% (*B. decoratus* sp. nov., MT333462, MT333463).

Discussion

Phylogeny and evolution of traits in *Bryodelphax*

Inter-generic tardigrade relationships are constantly being unravelled (Bertolani et al. 2014; Fujimoto et al. 2016; Gąsiorek et al. 2019a, b). Recently, Guil et al. (2019) proposed a new classification of Echiniscidae, with *Bryodelphax* included within Echiniscinae and having its own tribe Bryodelphaxini. Not only is such a proposal unjustified morphologically, as *Bryodelphax* is more similar to the *Pseudechiniscus*-like genera than to the *Echiniscus* lineage (Gąsiorek et al. 2018a), but, importantly, the current phylogenetic evidence is also not conclusive (different positions of the genus on echiniscid phylogenetic trees in Guil et al. 2019). In fact, the trait used to delimit putative Bryodelphaxini from Echiniscini, i.e. the presence of peribuccal cirrophores, is biased and unreliable – *Bryodelphax* has weakly outlined cirrophores due to the miniaturised body, but, essentially, the anatomy of cephalic cirri within both dubious tribes is identical. Therefore, the systematic distinction between Bryodelphaxini and Echiniscini is controversial and their status should be further verified. In terms of morphology, the genus should be currently recognised as a separate lineage of Echiniscidae, with the unsolved, long-standing problem of *Bryochoerus* (Kristensen 1987; Lisi et al. 2017; Gąsiorek 2018).

Regarding the phyletic relationships within the genus *Bryodelphax*, some intriguing conclusions can be drawn from the mapping of various phenotypic traits onto the phylogenetic tree (Fig. 1). Firstly, the division of the genus, based on the presence (*weglarskae* group) or absence (*parvulus* group) of ventral armature, has only practical significance for taxonomic purposes (see below), as the members of both groups are phylogenetically intermingled. This suggests that this trait is not conservative and its appearance should be regarded as convergent. Ventral plates are strongly sclerotised and evident in *B. amphoterus*, formerly affiliated within the *parvulus* group, which corroborates the supposition by Gąsiorek et al. (2017a) that these structures have been previously overlooked. Peculiarly, the reduction of ventral armature to plesiomorphic subcephalic and genital plate rows is known in *Bryodelphax* only in three Mediterranean species (*B. amphoterus*, *B. maculatus* and *B. nigripunctatus* sp. nov.).

Secondly, since the description of *B. maculatus*, dark epicuticular granules have received attention of taxonomists (Lisi et al. 2017; Kaczmarek et al. 2018). To date, these structures were recognised in eight *Bryodelphax* spp. during examination of comparative material (*B. aaseae*, *B. atlantis* Fontoura et al., 2008, *B. decoratus* sp. nov., *B. instabilis*, *B. kristenseni* Lisi et al., 2017, *B. maculatus*, *B. nigripunctatus* sp. nov. and *B. olszanowskii*). Although this trait was not described in many previous descriptions, our analysis indicated no granules in ten spp. (*B. amphoterus*, *B. arenosus*, *B. asiaticus*, *B.*

australasiaticus sp. nov., *B. brevidentatus*, *B. mateusi* (Fontoura, 1982), *B. meronensis*, *B. parvulus*, *B. tatrensis* (Węglarska, 1959) and *B. weglarskae*). Similarly to the traits described above, a glance at the distribution of species with dark epicuticular granules on the tree (Fig. 1) implies that this taxonomically-useful criterion bears no phylogenetic signal.

Thirdly, species exhibiting different modes of reproduction are scattered on the tree. Two of the three known dioecious *Bryodelphax* spp., *B. instabilis* and *B. nigripunctatus* sp. nov., are not directly related (Fig. 1). This pattern, that is parthenogenetic and dioecious taxa mixed on the tree, is consistent with recent data for *Paramacrobiotus* and *Milnesium* (Guidetti et al. 2019; Morek and Michalczyk 2020). However, most of the other echiniscid genera are more consistent in terms of the mode of reproduction (Kristensen 1987).

Last but not least, in contrast to phenotypic traits, geographic distribution of the analysed species suggests their limited dispersal abilities and seems to be a reliable predictor of phylogenetic affinities within the genus. This intriguing pattern has been recently shown in the genus *Milnesium* Doyère, 1840 by Morek and Michalczyk (2020). Considering the remote phyletic relationship and contrasting body sizes in the two groups (*Milnesium* comprises largest tardigrades), these results suggest that tardigrade species, in general, may have much more restricted geographic distributions than the "Everything is everywhere" hypothesis predicts (Beijerinck 1913).

It ought to be noted that the lengths of the tree branches in the case of the Oriental clade are considerably shorter than those for the Western Palaearctic clade (Fig. 1), whereas the taxa of both lineages are well-separated from each other (with the exception of *B. arenosus* and *Bryodelphax* sp. nov. from Seram, which requires more data to solve its phyletic relationship with other congeners). Deeper nodes in the Western Palaearctic clade may result from: (a) longer divergence time needed for cladogenesis in this region (e.g. Ricklefs 2004), (b) higher extinction rate in the tropics (e.g. Jablonski et al. 2006) or (c) from under-sampling of lineages in the Palaearctic (e.g. Chown and Gaston 2000). If the last possibility is excluded, then the observed pattern may mean that speciation could be more rapid in tropical tardigrades, as postulated by the tropical cradle biodiversity hypothesis, which assumes that young evolutionary lineages are prevalent in the tropics (Stebbins 1974; Stenseth 1984; Jablonski et al. 2006; Moreau and Bell 2013). A similar scenario was recently demonstrated for oribatid mites (Pachl et al. 2017), but a much greater sampling effort is required for *Bryodelphax* spp. in order to test this hypothesis.

Taxonomic key to the genus *Bryodelphax*

Since the last key by Fontoura et al. (2008), the number of described *Bryodelphax* species almost doubled (from 15 spp. considered valid in 2008 to 25 spp. gathered in the present contribution). Moreover, the 2008 key has several inadequacies: (I) three members of the *weglarskae* group (*B. iohannis*, *B. sinensis* and *B. weglarskae*) had an under-estimated number of ventral plates (nine instead of ten, six instead of seven and eight instead of nine, respectively); (II) *B. asiaticus* was delimited from *B. parvulus* by the absence of supplementary lateral platelets, but these structures are present in both species (Gąsiorek 2018). Our analysis of *B. amphoterus* paratypes revealed the presence of reduced, but evident ventral armature (formula II:2-2), thus the species belongs to the *weglarskae* group (Fig. 12). All these facts inclined us to present a new key allowing for the delimitation of females of the genus members at the adult life stage. The distinction between members of the *weglarskae* group (12 spp.) is rather straightforward, but the identification of species within the *parvulus* group (13 spp.) may pose a problem for beginner taxonomists. Consequently, we advise the greatest caution when identifying its members. Importantly, *B. lijiangensis* Yang, 2002 is designated as *nomen dubium* due to the insufficient description and the general habitus not conforming to the characteristics of the genus (trunk cirri in all lateral positions suggest its affinity to *Echiniscus*) and hence it is omitted from our key.

Key

1 Ventral plates present (the *weglarskae* group) 2
– Ventral plates absent (the *parvulus* group) 13
2(1) Two (subcephalic and genital) or three rows of ventral plates 3
– At least four rows of ventral plates 5
3(2) Ventral plate formula II:2-2, dark epicuticular granules absent, external claws with minute spurs ..... *B. amphoterus* (Durante Pasa & Maucci, 1975)
– Ventral plate formula different, dark epicuticular granules present, external claws spurless 4
4(3) Ventral plate formula III:2-2-1, entire venter and ventral plates covered with stripes of dark epicuticular granules, typical, short and stout *Bryodelphax* claws ..... *B. maculatus* Gąsiorek et al., 2017
– Ventral plate formula II/III:2-2-(1), only ventral plates covered with dark epicuticular granules, long and slender, *Pseudechiniscus*-like claws ..... *B. nigripunctatus* sp. nov.

5(2) Ventral plate rows composed of 1–2 plates each 6
– Ventral plate rows composed of at least three plates each (excluding the subcephalic row) 7
6(5) Ventral plate formula VIII:1-1-2-2-2-2-2-1, dentate collar IV present ..... *B. parvuspolaris* Kaczmarek et al., 2012
– Ventral plate formula VII:2-2-2-2-2-2-1, dentate collar IV absent ..... *B. sinensis* (Pilato, 1974)
7(5) Four plates in the subcephalic row 8
– Two or no plates in the subcephalic row 10
8(7) Eight rows of ventral plates, plates typically developed and with dark epicuticular granules ..... *B. olszanowskii* Kaczmarek et al., 2018*
– Seven rows of ventral plates, all plates faint and devoid of dark epicuticular granules 9
9(8) Ventral plate formula VII:4-4-2-4-2-2-1, dorsal plate margins uniformly thick and dark in PCM ..... *B. australasiaticus* sp. nov.
– Ventral plate formula VII:4-2-2-4-2-2-1, dorsal plate margins with separated epicuticular granules observable as dark points in PCM ..... *B. decoratus* sp. nov.
10(7) Ventral plate formula IX:2-2-5-2-4-2-2-2-1, cephalic cirri bifurcated at their tips ..... *B. weglarskae* (Pilato, 1972)
– Ventral plate formula different, cephalic cirri with a single tip 11
11(10) Ventral plate formula VII/IX:(2)-(1)-2/4-2-2/4-2-2-2-1, dioecious ..... *B. instabilis* Gąsiorek & Degma, 2018
– Ventral plate formula different, parthenogenetic 12
12(11) Ventral rows immediately before legs II and III, composed of 2 plates each ..... *B. iohannis* Bertolani et al., 1996
– Ventral rows immediately before legs II and III composed of 4 plates each 12
12(11) Ventral plate formula X:2-1-4-4-2-4-2-1-2-1, cirrus *A*/body length ratio at least 24% ..... *B. aaseae* Kristensen et al., 2010
– Ventral plate formula IX/X:2-(1)-4-4-2-4-2-1-2-1, cirrus *A*/body length ratio below 24% ..... *B. kristenseni* Lisi et al., 2017
13(1) Dentate collar IV present 14
– Dentate collar IV absent 19
14(13) Supplementary lateral plates absent ..... *B. brevidentatus* Kaczmarek et al., 2005
– Supplementary lateral plates present 15
15(14) Six supplementary lateral plates, more than ten teeth in the dentate collar ..... *B. alzirae* (du Bois-Reymond Marcus, 1944)
– Twelve supplementary lateral plates, fewer than ten teeth in the dentate collar 16
16(15) Papilla IV visible under LCM 17
– Papilla IV not visible under LCM 18
17(16) Endocuticular pillars in the scapular and the caudal (terminal) plate almost of the same size, pores evident and densely distributed on the anterior and lateral portions of the plates ..... *B. atlantis* Fontoura et al., 2008
– Endocuticular pillars in the scapular plate clearly smaller than pillars in the caudal (terminal) plate, pores evident only in the central portion of the paired plates ..... *B. meronensis* Pilato et al., 2010
18(16) Teeth of the dentate collar long and acute ..... *B. tatrensis* (Węglarska, 1959)
– Teeth of the dentate collar short and blunt ..... *B. mateusi* (Fontoura, 1982)
19(13) Pores/pseudopores absent, endocuticular pillars scarcely visible only in the caudal (terminal) plate, large depressions (fossae) in poorly defined rows ..... *B. dominicanus* (Schuster & Toftner, 1982)
– Pores/pseudopores present, endocuticular pillars visible on all dorsal plates, depressions (fossae) absent 20
20(19) Lateral portions of dorsal plates ornamented either with dark epicuticular granules or elevations ..... *B. arenosus* Gąsiorek, 2018
– Lateral portions of dorsal plates not ornamented 21
21(20) Supplementary lateral plates absent, internal claws spurless ..... *B. ortholineatus* (Bartoš, 1963)
– Supplementary lateral plates present, internal claws with spurs 22
22(21) Papilla IV visible under LCM ..... *B. crossotus* Grigarick et al., 1983
– Papilla IV not visible under LCM 23
23(22) The largest endocuticular pillars only in the central portion of the scapular plate ..... *B. parvulus* Thulin, 1928
– The largest endocuticular pillars in the central portions of the scapular and the caudal (terminal) plate and posterior portions of paired segmental plates ..... *B. asiaticus* Kaczmarek & Michalczyk, 2004

* Kaczmarek et al. (2018) defined the ventral plate formula as follows: VIII:2-1-1-2-2-2-2-2, i.e. not acknowledging another pair of ventrolateral plates as part of row I. These plates are added to the formula in the present contribution, resulting in the overall number of plates equal to four in the first ventral row, i.e. VIII:4-1-1-2-2-2-2-2.

Acknowledgements

Reinhardt M. Kristensen (University of Copenhagen), Roberto Guidetti (University of Modena and Reggio Emilia), Roberta Salmaso (Museum of Natural History of Verona) and Giovanni Pilato (University of Catania) are acknowledged for the loan of type material of some species. Alicja Witwicka, Artur Oczkowski and Łukasz Krzywański provided the moss samples or assisted in their collection. We are grateful to Sandra Claxton who consulted the morphology of individuals of *B. australasiaticus* sp. nov. from Australia and provided valuable microphotographs. Two reviewers, Matteo Vecchi and Łukasz Kaczmarek, kindly commented on the manuscript. The study and sampling were supported by the grant from the European Commission's (FP6) Integrated Infrastructure Initiative programme SYNTHESYS (grant no. DK-TAF-6332 to PG), National Science Centre (2019/33/N/NZ8/02777 to PG, supervised by ŁM), and by the Polish Ministry of Science and Higher Education via the Diamond Grant (DI2015 014945 to PG, supervised by ŁM). Some of the analyses were carried out with the equipment purchased from the *Sonata Bis* programme of the Polish National Science Centre (grant no. 2016/22/E/NZ8/00417 to ŁM). This work was also supported by the Slovak Research and Development Agency under the contract No. APVV-15-0147 (to PD). We owe our sincere thanks to the Museum für Naturkunde, Berlin, for covering the publication charge. The Authors declare no conflict of interest.

References

Bartoš E (1963) Die Tardigraden der chinesischen und javanischen Moosproben. Acta Societatis Zoologicae Bohemoslovenicae 27: 108–114.

Bertolani R, Guidi A, Rebecchi L (1996) Tardigradi della Sardegna e di alcune piccole isole circum-sarde. Biogeographia 18: 229–247. https://doi.org/10.21426/B618110456

Beijerinck MW (1913) De infusies en de ontdekking der backteriën. Jaarboek van de Koninklijke Akademie v. Wetenschappen. Amsterdam: Müller.

Bertolani R, Guidetti R, Marchioro T, Altiero T, Rebecchi L, Cesari M (2014) Phylogeny of Eutardigrada: New molecular data and their morphological support lead to the identification of new evolutionary lineages. Molecular Phylogenetics and Evolution 76: 110–126. https://doi.org/10.1016/j.ympev.2014.03.006

Casquet J, Thebaud C, Gillespie RG (2012) Chelex without boiling, a rapid and easy technique to obtain stable amplifiable DNA from small amounts of ethanol-stored spiders. Molecular Ecology Resources 12: 136–141. https://doi.org/10.1111/j.1755-0998.2011.03073.x

Chernomor O, von Haeseler A, Minh BQ (2016) Terrace aware data structure for phylogenomic inference from supermatrices. Systematic Biology 65: 997–1008. https://doi.org/10.1093/sysbio/syw037

Chown SL, Gaston KJ (2000) Areas, cradles and museums: the latitudinal gradient in species richness. Trends in Ecology & Evolution 15: 311–315. https://doi.org/10.1016/S0169-5347(00)01910-8

Claxton SK (2001) *Antechiniscus* in Australia: description of *Antechiniscus moscali* sp. n. and redescription of *Antechiniscus parvisentus* (Horning & Schuster, 1983) (Heterotardigrada: Echiniscidae). Zoologischer Anzeiger 240: 281–289. https://doi.org/10.1078/0044-5231-00035

Claxton SK (2004) The taxonomy and distribution of Australian terrestrial tardigrades. PhD Thesis, Macquarie University, Sydney, Australia, 618 pp.

Dastych H (1985) West Spitsbergen Tardigrada. Acta Zoologica Cracoviensia 28: 169–214.

Dastych H (1999) A new species of the genus *Mopsechiniscus* du Bois-Reymond Marcus, 1944 (Tardigrada) from the Venezuelan Andes. Acta biologica Benrodis 10: 91–101.

Doyère ML (1840) Mémorie sur les Tardigrades. Annales des Sciences Naturelles 14: 269–362.

du Bois-Reymond Marcus E (1944) Sobre tardígrados brasileiros. Comunicaciones Zoológicas del Museo de Historia Natural de Montevideo 1(13): 1–19.

Durante Pasa MV, Maucci W (1975) Tardigradi muscicoli dell'Istria con descrizione di due specie nuove. Memorie dell'Istituto Italiano di Idrobiologia 32(S): 69–91.

Fontoura AP (1982) Deux nouvelles espéces de Tardigrades muscicoles du Portugal. Publicações do Instituto de Zoologia "Dr. Augusto Nobre" 165: 5–19.

Fontoura P, Pilato G, Lisi O (2008) Echiniscidae (Tardigrada, Heterotardigrada) from Faial and Pico Islands, the Azores, with the description of two new species. Zootaxa 1693: 49–61. https://doi.org/10.11646/zootaxa.1693.1.4

Fontoura P, Bartels PJ, Jørgensen A, Kristensen RM, Hansen JG (2017) A dichotomous key to the genera of the Marine Heterotardigrades (Tardigrada). Zootaxa 4294: 1–45. https://doi.org/10.11646/zootaxa.4294.1.1

Fujimoto S, Jørgensen A, Hansen JG (2016) A molecular approach to arthrotardigrade phylogeny (Heterotardigrada, Tardigrada). Zoologica Scripta 46: 496–505. https://doi.org/10.1111/zsc.12221

Gąsiorek P (2018) New *Bryodelphax* species (Heterotardigrada: Echiniscidae) from Western Borneo (Sarawak), with new molecular data for the genus. Raffles Bulletin of Zoology 66: 371–381.

Gąsiorek P, Degma P (2018) Three Echiniscidae species (Tardigrada: Heterotardigrada) new to the Polish fauna, with the description of a new gonochoristic *Bryodelphax* Thulin, 1928. Zootaxa 4410: 77–96. https://doi.org/10.11646/zootaxa.4410.1.4

Gąsiorek P, Blagden B, Michalczyk Ł (2019a) Towards a better understanding of echiniscid intraspecific variability: A redescription of *Nebularmis reticulatus* (Murray, 1905) (Heterotardigrada: Echiniscoidea). Zoologischer Anzeiger 283: 242–255. https://doi.org/10.1016/j.jcz.2019.08.003

Gąsiorek P, Morek W, Stec D, Michalczyk Ł (2019b) Untangling the *Echiniscus* Gordian knot: paraphyly of the "*arctomys* group" (Heterotardigrada: Echiniscidae). Cladistics 35: 633–653. https://doi.org/10.1111/cla.12377

Gąsiorek P, Stec D, Morek W, Marnissi J, Michalczyk Ł (2017a) The tardigrade fauna of Tunisia, with an integrative description of *Bryodelphax maculatus* sp. nov. (Heterotardigrada: Echiniscidae). African Zoology 52: 77–89. https://doi.org/10.1080/15627020.2017.1297688

Gąsiorek P, Stec D, Morek W, Michalczyk Ł (2017b) An integrative redescription of *Echiniscus testudo* (Doyère, 1840), the nominal taxon for the class Heterotardigrada (Ecdysozoa: Panarthropoda: Tardigra-

da). Zoologischer Anzeiger 270: 107–122. https://doi.org/10.1016/j.jcz.2017.09.006

Gąsiorek P, Stec D, Zawierucha K, Kristensen RM, Michalczyk Ł (2018b) Revision of *Testechiniscus* Kristensen, 1987 (Heterotardigrada: Echiniscidae) refutes the polar-temperate distribution of the genus. Zootaxa 4472: 261–297. https://doi.org/10.11646/zootaxa.4472.2.3

Gąsiorek P, Suzuki AC, Kristensen RM, Lachowska-Cierlik D, Michalczyk Ł (2018a) Untangling the *Echiniscus* Gordian knot: *Stellariscus* gen. nov. (Heterotardigrada: Echiniscidae) from Far East Asia. Invertebrate Systematics 32: 1234–1247. https://doi.org/10.1071/IS18023

Grigarick AA, Schuster RO, Nelson DR (1983) Heterotardigrada of Venezuela (Tardigrada). Pan-Pacific Entomologist 59: 64–77.

Gross V, Treffkorn S, Reichelt J, Epple L, Lüter C, Mayer G (2019) Miniaturization of tardigrades (water bears): Morphological and genomic perspectives. Arthropod Structure & Development 48: 12–19. https://doi.org/10.1016/j.asd.2018.11.006

Guidetti R, Cesari M, Bertolani R, Altiero T, Rebecchi L (2019) High diversity in species, reproductive modes and distribution within the *Paramacrobiotus richtersi* complex (Eutardigrada, Macrobiotidae). Zoological Letters 5: 1. https://doi.org/10.1186/s40851-018-0113-z

Guidetti R, Rebecchi L, Bertolani R, Jönsson KI, Kristensen RM, Cesari M (2016) Morphological and molecular analyses on *Richtersius* (Eutardigrada) diversity reveal its new systematic position and lead to the establishment of a new genus and a new family within Macrobiotoidea. Zoological Journal of the Linnean Society 178: 834–845. https://doi.org/10.1111/zoj.12428

Guil N (2002) Diversity and distribution of tardigrades (Bilateria, Tardigrada) from the Iberian Peninsula, Balearic Islands and Chafarinas Islands. Graellsia 58: 75–94. https://doi.org/10.3989/graellsia.2002.v58.i2.279

Guil N, Jørgensen A, Kristensen R (2019) An upgraded comprehensive multilocus phylogeny of the Tardigrada tree of life. Zoologica Scripta 48: 120–137. https://doi.org/10.1111/zsc.12321

Hall TA (1999) BioEdit: a user-friendly biological sequence alignment editor and analysis program for Windows 95/98/NT. Nucleic Acids Symposium Series 41: 95–98.

Hoang DT, Chernomor O, von Haeseler A, Minh BQ, Vinh LS (2018) UFBoot2: Improving the ultrafast bootstrap approximation. Molecular Biology and Evolution 35: 518–522. https://doi.org/10.1093/molbev/msx281

Jablonski D, Roy K, Valentine JW (2006) Out of the tropics: Evolutionary dynamics of the latitudinal diversity gradient. Science 314: 102–106. https://doi.org/10.1126/science.1130880

Jørgensen A, Boesgaard TM, Møbjerg N, Kristensen RM (2014) The tardigrade fauna of Australian marine caves: With descriptions of nine new species of Arthrotardigrada. Zootaxa 3802: 401–443. https://doi.org/10.11646/zootaxa.3802.4.1

Kaczmarek Ł, Michalczyk Ł (2004) A new species *Bryodelphax asiaticus* (Tardigrada: Heterotardigrada: Echiniscidae) from Mongolia (Central Asia). Raffles Bulletin of Zoology 52: 599–602.

Kaczmarek Ł, Michalczyk Ł, Degma P (2005) A new species of Tardigrada *Bryodelphax brevidentatus* sp. nov. (Heterotardigrada: Echiniscidae) from China (Asia). Zootaxa 1080: 33–45. https://doi.org/10.11646/zootaxa.1080.1.3

Kaczmarek Ł, Zawierucha K, Smykla J, Michalczyk Ł (2012) Tardigrada of the Revdalen (Spitsbergen) with the descriptions of two new species: *Bryodelphax parvuspolaris* (Heterotardigrada) and *Isohypsibius coulsoni* (Eutardigrada). Polar Biology 35: 1013–1026. https://doi.org/10.1007/s00300-011-1149-0

Kaczmarek Ł, Parnikoza I, Gawlak M, Esefeld J, Peter H-U, Kozeretska I, Roszkowska M (2018) Tardigrades from *Larus dominicanus* Lichtenstein, 1823 nests on the Argentine Islands (maritime Antarctic). Polar Biology 41: 283–301. https://doi.org/10.1007/s00300-017-2190-4

Kalyaanamoorthy S, Minh BQ, Wong TKF, von Haeseler A, Jermiin LS (2017) ModelFinder: Fast model selection for accurate phylogenetic estimates. Nature Methods 14: 587–589. https://doi.org/10.1038/nmeth.4285

Katoh K, Toh H (2008) Recent developments in the MAFFT multiple sequence alignment program. Briefings in Bioinformatics 9: 286–298. https://doi.org/10.1093/bib/bbn013

Katoh K, Misawa K, Kumar K, Mitaya T (2002) MAFFT: a novel method for rapid multiple sequence alignment based on fast Fourier transform. Nucleic Acids Research 30: 3059–3066. https://doi.org/10.1093/nar/gkf436

Kristensen RM (1987) Generic revision of the Echiniscidae (Heterotardigrada), with a discussion of the origin of the family. In: Bertolani R (Ed.) Biology of Tardigrades. Selected Symposia and Monographs U.Z.I. 1: 261–335.

Kristensen RM, Michalczyk Ł, Kaczmarek Ł (2010) The first record of the genus *Bryodelphax* (Tardigrada: Heterotardigrada: Echiniscidae) from Easter Island, Rapa Nui (Pacific Ocean, Chile) with the description of a new species, *Bryodelphax aaseae*. Zootaxa 2343: 45–56. https://doi.org/10.11646/zootaxa.2343.1.4

Kumar S, Stecher G, Taura K (2016) MEGA7: Molecular Evolutionary Genetics Analysis version 7.0 for bigger datasets. Molecular Biology and Evolution 33: 1870–1874. https://doi.org/10.1093/molbev/msw054

Lanfear R, Calcott B, Ho SY, Guindon S (2012) PartitionFinder: combined selection of partitioning schemes and substitution models for phylogenetic analyses. Molecular Biology and Evolution 29: 1695–1701. https://doi.org/10.1093/molbev/mss020

Lanfear R, Frandsen PB, Wright AM, Senfeld T, Calcott B (2016) PartitionFinder 2: new methods for selecting partitioned models of evolution for molecular and morphological phylogenetic analyses. Molecular Biology and Evolution 34: 772–773. https://doi.org/10.1093/molbev/msw260

Lisi O, Daza A, Londoño R, Quiroga S (2017) Echiniscidae from the Sierra Nevada de Santa Marta, Colombia, new records and a new species of *Bryodelphax* Thulin, 1928 (Tardigrada). ZooKeys 703: 1–14. https://doi.org/10.3897/zookeys.703.12537

Marcus E (1927) Zur Anatomie und Ökologie mariner Tardigraden. Zoologische Jahrbücher. Abteilung für Systematik, Ökologie und Geographie der Tiere 53: 487–558.

Maucci W (1979) I *Pseudechiniscus* del gruppo *cornutus*, con descrizione di una nuova specie (Tardigrada, Echiniscidae). Zeszyty Naukowe Uniwersytetu Jagiellońskiego 25: 107–124.

Maucci W (1996) Tardigrada of the Arctic tundra with descriptions of two new species. Zoological Journal of the Linnean Society 116: 185–204. https://doi.org/10.1006/zjls.1996.0016

McInnes SJ (1994) Zoogeographic distribution of terrestrial/freshwater tardigrades from current literature. Journal of Natural History 28: 257–352. https://doi.org/10.1080/00222939400770131

Michalczyk, Ł, Kaczmarek Ł (2013) The Tardigrada Register: a comprehensive online data repository for tardigrade taxonomy. Jour-

nal of Limnology 72(S1): 175–181. https://doi.org/10.4081/jlimnol.2013.s1.e22

Mironov SV, Dabert J, Dabert M (2012) A new feather mite species of the genus *Proctophyllodes* Robin, 1877 (Astigmata: Proctophyllodidae) from the long-tailed tit *Aegithalos caudatus* (Passeriformes: Aegithalidae): morphological description with DNA barcode data. Zootaxa 3253: 54–61. https://doi.org/10.11646/zootaxa.3253.1.2

Moreau CS, Bell CD (2013) Testing the museum versus cradle tropical biological diversity hypothesis: phylogeny, diversification, and ancestral biogeographic range evolution of the ants. Evolution 67: 2240–2257. https://doi.org/10.1111/evo.12105

Morek W, Gąsiorek P, Stec D, Blagden B, Michalczyk Ł (2016) Experimental taxonomy exposes ontogenetic variability and elucidates the taxonomic value of claw configuration in *Milnesium* Doyère, 1840 (Tardigrada: Eutardigrada: Apochela). Contributions to Zoology 85: 173–200. https://doi.org/10.1163/18759866-08502003

Morek W, Michalczyk Ł (2020) First extensive multilocus phylogeny of the genus *Milnesium* (Tardigrada) reveals no congruence between genetic markers and morphological traits. Zoological Journal of the Linnean Society 188: 681–693. https://doi.org/10.1093/zoolinnean/zlz040

Nei M, Kumar S (2000) Molecular Evolution and Phylogenetics. Oxford University Press, Oxford, 348 pp.

Nelson DR, Guidetti R, Rebecchi L (2015) Phylum Tardigrada. Chapter 17. In: Thorp JH, Rogers DC (Eds) Thorp and Covich's Freshwater Invertebrates. Academic Press, Cambridge, 347–380. https://doi.org/10.1016/B978-0-12-385026-3.00017-6

Nguyen L-T, Schmidt HA, von Haeseler A, Minh BQ (2015) IQ-TREE: A fast and effective stochastic algorithm for estimating maximum likelihood phylogenies. Molecular Biology and Evolution 32: 268–274. https://doi.org/10.1093/molbev/msu300

Pachl P, Lindl AC, Krause A, Scheu S, Schaefer I, Maraun M (2017) The tropics as an ancient cradle of oribatid mite diversity. Acarologia 57: 309–322. https://doi.org/10.1051/acarologia/20164148

Pilato G (1972) Prime osservazioni sui tardigradi delle Isole Egadi. Bollettino delle Sedute della Accademia Gioenia di Scienze Naturali in Catania, serie IV 11: 111–124.

Pilato G (1974) Tre nuove specie di tardigradi muscicoli di Cina. Animalia 1: 59–68.

Pilato G, Fontoura P, Lisi O, Beasley C (2008) New description of *Echiniscus scabrospinosus* Fontoura, 1982, and description of a new species of *Echiniscus* (Heterotardigrada) from China. Zootaxa 1856: 41–54. https://doi.org/10.11646/zootaxa.1856.1.4

Pilato G, Lisi O, Binda MG (2010) Tardigrades of Israel with description of four new species. Zootaxa 2665: 1–28. https://doi.org/10.11646/zootaxa.2665.1.1

Rambaut A, Drummond AJ, Xie D, Baele G, Suchard MA (2018) Posterior summarisation in Bayesian phylogenetics using Tracer 1.7. Systematic Biology 67: 901–904. https://doi.org/10.1093/sysbio/syy032

Richters F (1904) Isländische Tardigraden. Zoologischer Anzeiger 28: 373–377.

Richters F (1926) Tardigrada. Handbuch der Zoologie (Vol. 3). de Gruyter, Berlin and Leipzig, 58–61.

Ricklefs RE (2004) Cladogenesis and morphological diversification in passerine birds. Nature 430: 338–341. https://doi.org/10.1038/nature02700

Ronquist F, Huelsenbeck JP (2003) MrBayes 3: Bayesian phylogenetic inference under mixed models. Bioinformatics 19: 1572–1574. https://doi.org/10.1093/bioinformatics/btg180

Schuster RO, Toftner EC (1982) Dominican Republic Tardigrada. Proceedings of the Third International Symposium on the Tardigrada, East Tennessee State University Press, Johnson City, Tennessee, 221–236.

Srivathsan A, Meier R (2012) On the inappropriate use of Kimura–2–parameter (K2P) divergences in the DNA-barcoding literature. Cladistics 28: 190–194. https://doi.org/10.1111/j.1096-0031.2011.00370.x

Stebbins GL (1974) Flowering plants: evolution above the species level. The Belknap Press of Harvard University Press, Cambridge, 480 pp. https://doi.org/10.4159/harvard.9780674864856

Stec D, Smolak R, Kaczmarek Ł, Michalczyk Ł (2015) An integrative description of *Macrobiotus paulinae* sp. nov. (Tardigrada: Eutardigrada: Macrobiotidae: *hufelandi* group) from Kenya. Zootaxa 4052: 501–526. https://doi.org/10.11646/zootaxa.4052.5.1

Stec D, Zawierucha K, Michalczyk Ł (2017) An integrative description of *Ramazzottius subanomalus* (Biserov, 1985) (Tardigrada) from Poland. Zootaxa 4300: 403–420. https://doi.org/10.11646/zootaxa.4300.3.4

Stenseth NC (1984) The tropics: cradle or museum? Oikos 43: 417–420. https://doi.org/10.2307/3544168

Thulin G (1928) Über die Phylogenie und das System der Tardigraden. Hereditas 11: 207–266. https://doi.org/10.1111/j.1601-5223.1928.tb02488.x

Trifinopoulos J, Nguyen L-T, von Haeseler A, Minh BQ (2016) W-IQ-TREE: a fast online phylogenetic tool for maximum likelihood analysis. Nucleic Acids Research 44: 232–235. https://doi.org/10.1093/nar/gkw256

Vaidya G, Lohman DJ, Meier R (2011) SequenceMatrix: concatenation software for the fast assembly of multi-gene datasets with character set and codon information. Cladistics 27: 171–180. https://doi.org/10.1111/j.1096-0031.2010.00329.x

Węglarska B (1959) Niesporczaki (Tardigrada) Polski I. Niesporczaki województwa krakowskiego. Acta Zoologica Cracoviensia 4: 699–745.

Wełnicz W, Grohme MA, Kaczmarek Ł, Schill RO, Frohme M (2011) ITS-2 and 18S rRNA data from *Macrobiotus polonicus* and *Milnesium tardigradum* (Eutardigrada, Tardigrada). Journal of Zoological Systematics and Evolutionary Research 49(S1): 34–39. https://doi.org/10.1111/j.1439-0469.2010.00595.x

Yang T (2002) The Tardigrades from some mosses of Lijiang County in Yunnan Province (Heterotardigrada: Echiniscidae; Eutardigrada: Parachela: Macrobiotidae, Hypsibiidae). Acta Zootaxonomica Sinica 27: 53–64.

Zeller C (2010) Untersuchung der Phylogenie von Tardigraden anhand der Genabschnitte 18S rDNA und Cytochrom c Oxidase Untereinheit 1 (COX I). MSc Thesis, Technische Hochschule Wildau, Germany, 105 pp.